JOURNAL OF PETROLOGY | VOLUME 45 | NUMBER 12 | PAGES 2531–2553 | 2004 | doi:10.1093/petrology/egh080

Melt Inclusions in Primitive Olivine Phenocrysts: the Role of Localized Reaction Processes in the Origin of Anomalous Compositions

LEONID V. DANYUSHEVSKY[1]*, ROMAN A. J. LESLIE[1], ANTHONY J. CRAWFORD[1] AND PATRICIA DURANCE[1,2]

[1]SCHOOL OF EARTH SCIENCES AND CENTRE FOR ORE DEPOSIT RESEARCH, UNIVERSITY OF TASMANIA, PRIVATE BAG 79, HOBART, TAS. 7001, AUSTRALIA

[2]SCHOOL OF GEOSCIENCES, PO BOX 28E, MONASH UNIVERSITY, VIC. 3800, AUSTRALIA

RECEIVED FEBRUARY 2, 2004; ACCEPTED SEPTEMBER 22, 2004
ADVANCE ACCESS PUBLICATION NOVEMBER 5, 2004

Melt inclusions are small portions of liquid trapped by growing crystals during magma evolution. Recent studies of melt inclusions have revealed a large range of unusual major and trace element compositions in phenocrysts from primitive mantle-derived magmatic rocks [e.g. in high-Fo olivine (Fo $>$ *~85 mol %), spinel, high-An plagioclase]. Inclusions in phenocrysts crystallized from more evolved magmas (e.g. olivine Fo* $<$ *~85 mol %), are usually compositionally similar to the host lavas. This paper reviews the chemistry of melt inclusions in high-Fo olivine phenocrysts focusing on those with anomalous major and trace element contents from mid-ocean ridge and subduction-related basalts. We suggest that a significant portion of the anomalous inclusion compositions reflects localized, grain-scale dissolution–reaction–mixing (DRM) processes within the magmatic plumbing system. The DRM processes occur at the margins of primitive magma bodies, where magma is in contact with cooler wall rocks and/or pre-existing semi-solidified crystal mush zones (depending on the specific environment). Injection of hotter, more primitive magma causes partial dissolution (incongruent melting) of the mush-zone phases, which are not in equilibrium with the primitive melt, and mixing of the reaction products with the primitive magma. Localized rapid crystallization of high-Fo olivines from the primitive magma may lead to entrapment of numerous large melt inclusions, which record the DRM processes in progress. In some magmatic suites melt inclusions in primitive phenocrysts may be naturally biased towards the anomalous compositions. The occurrence of melt inclusions with unusual compositions does not necessarily imply the existence of new geologically significant magma types and/or melt-generation processes, and caution should be exercised in their interpretation.*

KEY WORDS: *melt inclusions; olivine; geochemistry; mush zones; MORB; subduction-related magmas*

INTRODUCTION

Melt inclusions ('inclusions' hereafter), are small portions of magma trapped by crystals growing during magma evolution that represent 'snapshots' of the crystallization environment. Such inclusions may be particularly useful in studies of primitive mantle-derived magmas that are frequently modified prior to eruption by fractionation processes within the magmatic plumbing system.

It is now well recognized that the original compositions of inclusions are readily modified after trapping by crystallization of the host phase on the walls and other daughter phases within the inclusions prior to and during eruption (e.g. Roedder, 1979, 1984). Such modifications can be reversed either by laboratory reheating of the inclusions or numerical modelling of crystallization processes within them (e.g. Sobolev *et al.*, 1980; Sinton *et al.*, 1993; Danyushevsky *et al.*, 2002*b*).

A second mechanism that acts to modify inclusion compositions after trapping is re-equilibration with the host phenocryst and/or external magma (e.g. Roedder, 1979; Qin *et al.*, 1992; Tait, 1992; Danyushevsky *et al.*,

*Corresponding author. Telephone: +61-3-62262429. Fax: +61-3-62262547. E-mail: L.Dan@utas.edu.au

2000*a*; Gaetani & Watson, 2000; Massare *et al.*, 2002). In high-Fo olivine phenocrysts from primitive mantle-derived magmas such processes include loss of volatiles from inclusions and their Fe–Mg exchange with the host. Techniques for minimizing the effects of such modifications, and their use to infer the cooling paths of evolving magmas, have been discussed by Gaetani & Watson (2000) and Danyushevsky *et al.* (2002*b*, 2002*c*).

The reconstruction of originally trapped melt compositions is not the only important issue pertinent to melt inclusion studies. Another issue relates to the critical assessment of the origin of what has actually been sampled by the host phenocryst during inclusion formation. In this paper we address whether melt inclusions are always samples of geologically significant melt bodies within the magmatic plumbing system, or whether in some cases the host phenocryst may sample localized grain-scale environments.

Recent studies of inclusions have revealed a large range of unusual major and trace element compositions in phenocrysts from primitive mantle-derived magmatic rocks. Although these unusual inclusions occur mainly in high-Fo olivine, they have also been reported in spinel (e.g. Sigurdsson *et al.*, 2000) and high-An plagioclase (e.g. Nielsen *et al.*, 1995). In terms of major elements, a common feature of the more anomalous inclusion compositions in olivine is their high CaO content and CaO/Al_2O_3 ratios (e.g. Schiano *et al.*, 2000). Although found in samples from different tectonic settings, this feature is most pronounced in inclusions from subduction-related volcanic rocks (Fig. 1). In general, high-CaO inclusions in mid-ocean ridge basalts (MORB) and ocean-island basalts (OIB) have higher SiO_2, whereas the high-CaO inclusions in the subduction-related lavas have lower SiO_2 than the host lavas (e.g. Kogiso & Hirschmann, 2001). Figure 1 also demonstrates that anomalous characteristics are predominantly found in inclusions in high-Fo olivine phenocrysts (Fo $>$ $\sim$85). Inclusions in less forsteritic olivine, when present in the same samples, are usually compositionally similar to the host lavas (Fig. 1).

A common feature of inclusions from different tectonic settings, particularly in MORB and back-arc basin basalts (BABB), is the large range of concentrations of strongly incompatible elements (SIE), such as Ba, Rb, Th, U, Ta, Nb, K and La. The range of SIE contents in inclusions within a magmatic suite, or even within a single sample and, in some cases, within a single grain, can exceed the range recorded by the host lavas by more than an order of magnitude (e.g. Sobolev *et al.*, 1992, 2000; Sobolev & Shimizu, 1993; Gurenko & Chaussidon, 1995; Kamenetsky *et al.*, 1997, 1998; Shimizu, 1998; Danyushevsky *et al.*, 2003). At the same time, concentrations of moderately incompatible elements (MIE, i.e. Sm, Eu, Ti, Gd, Dy, Er, Y, Yb, Lu) in such inclusions are usually more uniform and similar to the compositions of the host lavas, resulting in large variations of SIE/MIE ratios in the inclusions.

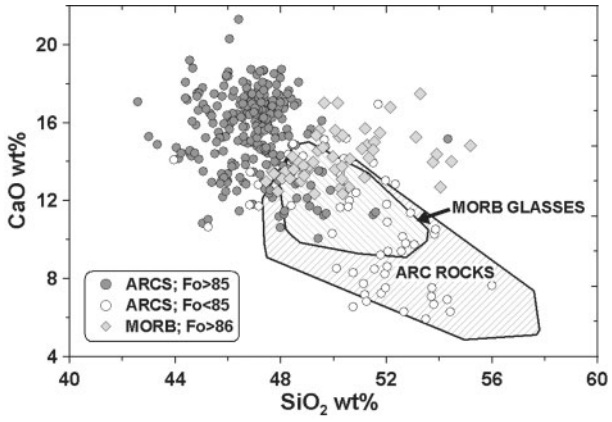

Fig. 1. CaO and SiO_2 contents (wt %) in olivine-hosted melt inclusions from primitive MORB and subduction-related lavas that contain high-CaO inclusion compositions. Melt inclusions from samples that do not contain high-CaO inclusions are not shown. MORB melt inclusion compositions are from Gurenko & Chaussidon (1995), Kamenetsky *et al.* (1997, 1998) and Danyushevsky *et al.* (2003). Subduction-related melt inclusion compositions are from Kamenetsky & Clocchiatti (1996), Della-Pasqua (1997), Della-Pasqua & Varne (1997), Gioncada *et al.* (1998), Sisson & Bronto (1998), Metrich *et al.* (1999), Schiano *et al.* (2000) and our unpublished data. The 'MORB glasses' field includes MORB pillow-rim glasses with MgO >8 wt % from different localities from the Smithsonian Institution catalogue (Melson *et al.*, 2002; http://www.nmnh.si.edu/minsci/research/glass/index.htm) and our unpublished data. The 'Arc rocks' field includes whole-rock compositions of subduction-related lava suites from the same localities as the melt inclusions.

Two general types of relationship between the SIE concentrations of inclusions and their host lavas can be identified for MORB and BABB samples. In areas where SIE-enriched and SIE-depleted lavas are found in close proximity to each other, inclusions with both characteristics may be found in a single rock sample (e.g. Shimizu, 1998). In other areas where the host lavas have relatively uniform SIE compositions, a continuum of SIE concentrations from highly depleted to variably enriched is found in inclusions from a single rock sample (e.g. Sobolev & Shimizu, 1993; Gurenko & Chaussidon, 1995; Kamenetsky *et al.*, 1998; Danyushevsky *et al.*, 2003).

In MORB, most inclusions, either SIE-depleted or SIE-enriched, have typically smooth primitive mantle-normalized incompatible element patterns (Fig. 2a). However, in some samples a subset of inclusions display unusual geochemical characteristics such as large positive Sr anomalies (Fig. 2a), which are not recorded in the host lavas (e.g. Kamenetsky *et al.*, 1998; Danyushevsky *et al.*, 2003).

The compositional diversity in primitive inclusions has been interpreted to originate from melt-generation processes in the mantle (e.g. Sobolev & Shimizu, 1993), channelized melt transport in the mantle

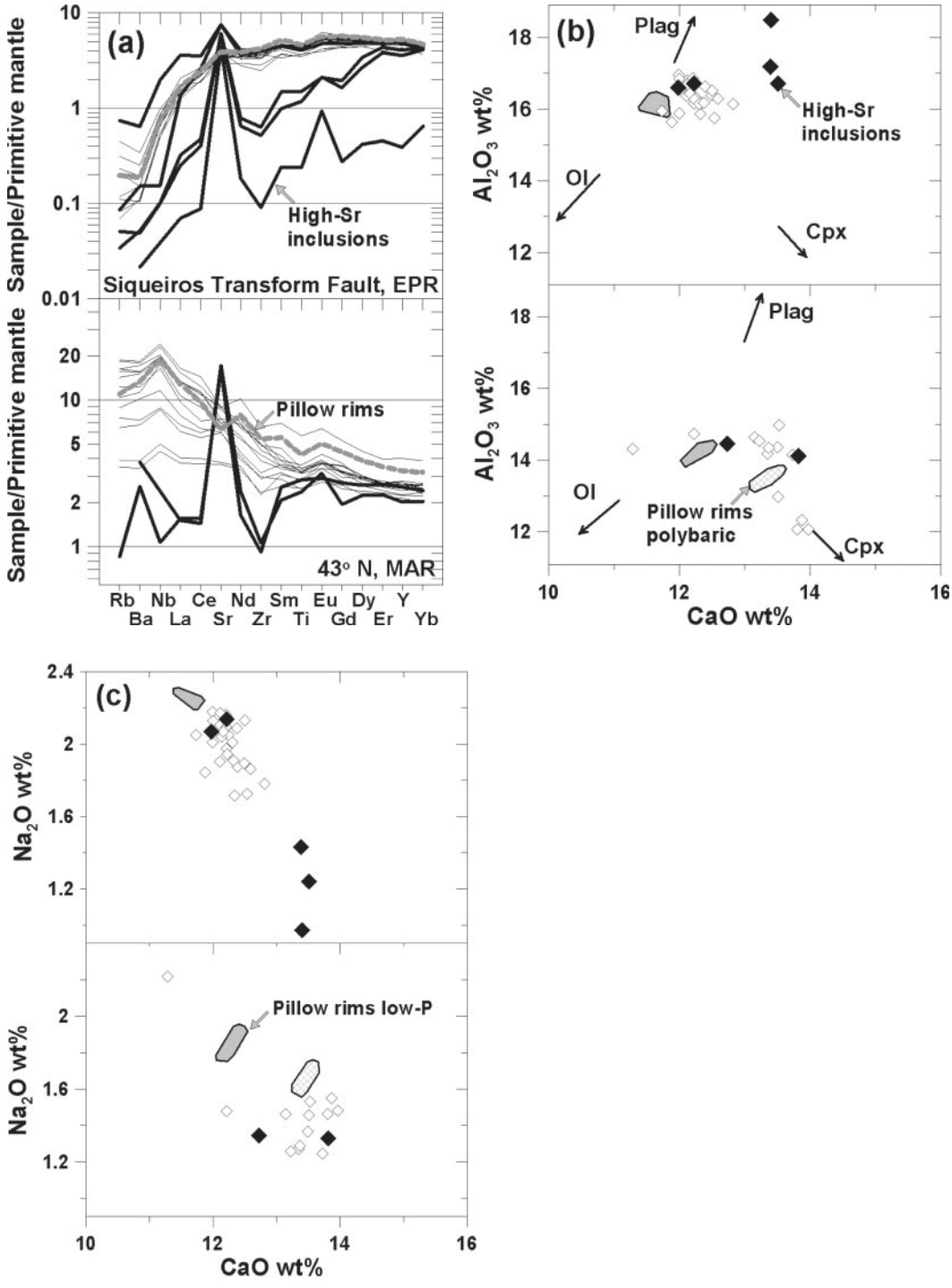

Fig. 2. Examples of anomalous melt inclusions in high-Fo olivine phenocrysts from MORB. All compositions are recalculated to correct for fractionation as described in the Appendix. (a) Primitive mantle-normalized incompatible element contents of melt inclusions from samples ALV-2384-3, Siqueiros Transform Fault, East Pacific Rise (EPR) (Danyushevsky *et al.*, 2003) and AII32-12-7, 43°N, Mid-Atlantic Ridge (MAR) (Kamenetsky *et al.*, 1998). Bold black lines show inclusions with positive Sr anomalies. Thick dashed grey lines show the trace element patterns of pillow-rim glasses of the host lavas. All trace element data have been normalized to the primitive mantle values of Sun & McDonough (1989). (b, c) The CaO, Al_2O_3 and Na_2O contents in melt inclusions from (a). Filled diamonds represent inclusions with Sr anomalies from (a). The shaded fields show fractionation-corrected compositions of pillow-rim glasses from both suites (Shibata *et al.*, 1979; Kamenetsky *et al.*, 1998; Danyushevsky *et al.*, 2003). For the 43°N MAR glasses correction for fractionation has been performed assuming both low-pressure and polybaric fractionation of primitive magmas (see Appendix for calculation details). Arrows labelled Ol, Plag and Cpx in (b) point to average compositions of primitive MORB olivine, plagioclase and clinopyroxene phenocrysts, respectively. (See text for discussion.)

(Spiegelman & Kelemen, 2003), fine-scale mantle heterogeneity (Sobolev *et al.*, 2000), or assimilation of wall-rock material in the magmatic plumbing system (e.g. Kent *et al.*, 2002; Lassiter *et al.*, 2002).

There are two important assumptions common to all these interpretations.

(1) The host lavas do not preserve the initial variety of melt compositions, as a result of extensive mixing of distinct melts in the plumbing system. This mixing occurs relatively early in the crystallization history of a magma, explaining the rarity of unusual inclusion compositions in the more evolved phenocrysts that formed when mixing is complete.

(2) Inclusions represent snapshots of relatively large-volume, geologically significant melt bodies that exist in the volcanic plumbing system during crystal growth.

Here we present an alternative view for the origin of anomalous melt inclusion compositions. From a detailed description of such inclusion compositions from MORB and subduction-related samples, we propose that a significant portion of these compositions may not represent geologically significant melts, but instead reflect localized, grain-scale reaction processes within the magmatic plumbing system. Similar ideas have been presented by Bedard *et al.* (2000). We also suggest that in some magmatic suites inclusions in primitive phenocrysts are naturally biased towards such anomalous compositions. This paper does not aim to provide a quantitative model that can account for the origin of every anomalous inclusion composition. Instead, we present a conceptual approach for explaining the origin of inclusions with anomalous composition.

SAMPLES AND ANALYTICAL TECHNIQUES

Ideas presented in this paper originated from studies of the geochemistry, mineralogy and melt inclusions in olivine phenocrysts from four magmatic suites as follows.

(1) The 5–3 Ma shoshonites from three volcanic centres in Fiji (Tavua Volcano, samples EL-8, EL-9, EL-10; Vatu-i-Cake Island, sample VT-3; Astrolabe Islands). Altogether we have studied ~300 olivine-hosted melt inclusions from nine samples. Fijian shoshonites display strong subduction-related geochemistry with high ratios of large ion lithophile elements to high field strength elements (LILE/HFSE) (e.g. Gill & Whelan, 1989). A detailed description of these rocks will be published elsewhere (Leslie *et al.*, in preparation).

(2) Zero age arc tholeiites from two submarine volcanoes from the Hunter Ridge, southern termination of the North Fiji back-arc basin (~150 melt inclusions in olivine phenocrysts from samples D2-1 and D3-1 have been studied). A detailed description of these rocks will be published elsewhere (Durance-Sie *et al.*, in preparation).

(3) Zero age MORB from the Siqueiros Transform Fault, East Pacific Rise (EPR) (Danyushevsky *et al.*, 2003).

(4) The 2–0 Ma boninites from the northern termination of the Tonga–Kermadec Arc (Danyushevsky *et al.*, 1995).

Experimental reheating of melt inclusions

Most melt inclusions in olivine phenocrysts in samples from Fiji and the Hunter Ridge are recrystallized. Such inclusions have been reheated to remelt the daughter crystals inside them and quenched to glass prior to analysis. All experiments have been conducted under visual control using a specially designed low-inertia heating stage (Sobolev *et al.*, 1980). Melt inclusions from the Fijian shoshonites were kept at high temperatures (>1050°C) for ~5 min. Melt inclusions from Hunter Ridge tholeiites were kept at high temperature for 1–2 min. A detailed description of experimental techniques has been given by Danyushevsky *et al.* (2002*b*).

Analytical techniques

Major and minor elements in glasses, plagioclase and olivine phenocrysts were analysed using Cameca SX50 and SX100 electron microprobes at the University of Tasmania. Glass and plagioclase were analysed at 15 kV, 20 nA, and a beam size of 5 μm. International standard USNM 111240/2 (basaltic glass VG2) and USNM 119500 (plagioclase) from Jarosewich *et al.* (1980) were used as the primary and secondary standard analysed throughout analytical sessions. Counting times for Na, Mg, Al, Si, Ca and Mn were 10 s for the peaks and 5 s for the backgrounds (10/5) on both sides. For Ti and Fe, counting times were 20/10, and for K, P and Cr they were 60/30. Olivine was analysed at 15 kV, 30 nA, and a beam size of 1–2 μm. International standards USNM 111312/444 (San Carlos olivine) from Jarosewich *et al.* (1980) were used as the primary and secondary standard analysed throughout analytical sessions. Counting times for Mg, Si and Fe were 20/10; for Ca, Cr, Ni, and Mn they were 30/15. Each electron microprobe analysis presented in this paper is an average of two or three individual spots. Accuracy of the electron microprobe analysis in the above conditions varies from 2% for major elements to as much as 100% for absolute contents of 0·01 wt %.

Trace element concentrations in plagioclase were analysed by laser ablation inductively coupled plasma mass spectrometry at the University of Tasmania. This instrumentation comprises a New Wave Research UP213 Md-YAG (213 nm) laser coupled to an Agilent 4500 quadrupole mass spectrometer. Analyses were performed by ablating 55 μm diameter spots at a rate of 10 shots/s.

Data reduction was undertaken according to standard methods (Longerich *et al.*, 1996) using the NIST612 glass as a primary reference material and the USGS BCR2 g glass as a secondary reference material.

The complete major and trace element dataset may be downloaded from the *Journal of Petrology* website at http://www.petrology.oupjournals.org

ANOMALOUS MELT INCLUSIONS FROM MORB

In a number of MORB samples with typically smooth primitive mantle-normalized incompatible element patterns, inclusions in high-Fo olivine phenocrysts display a large range of SIE concentrations and also have positive Sr anomalies that are not observed in the host lavas (note that Sr anomalies do not occur in every MORB sample where inclusions display a large range of SIE contents, e.g. Sobolev, 1996). Figure 2a illustrates two such samples, one SIE-depleted (sample ALV-2384-3, Siqueiros Transform Fault, EPR; Perfit *et al.*, 1996; Danyushevsky *et al.*, 2003) and one SIE-enriched [sample 12-7, 43°N Mid-Atlantic Ridge (MAR); Kamenetsky *et al.*, 1998]. Within a sample, Sr anomalies are usually present in, but are not restricted to, the most SIE-depleted inclusions (Fig. 2a). Such inclusions are referred to as high-Sr inclusions hereafter. Within a sample, high-Sr inclusions usually represent only a small part of the inclusion population (e.g. <3% of inclusions in the Siqueiros sample have Sr anomalies; Danyushevsky *et al.*, 2003; Fig. 2a).

High-Sr melt inclusions from samples ALV-2384-3 and 12-7

Danyushevsky *et al.* (2003) have considered in detail the origin of SIE-depleted, high-Sr inclusions from sample ALV-2384-3. These inclusions have the highest Al_2O_3 and CaO contents and the lowest Na_2O and TiO_2 contents within the suite (Fig. 2b and c), and are associated with aluminous spinels with variable Cr_2O_3 content. Danyushevsky *et al.* (2003) have interpreted these inclusions to represent the products of reactions between plagioclase (± clinopyroxene) and hot primitive MORB melt that is undersaturated in plagioclase and clinopyroxene at crustal pressures. Such reactions occur on a local scale (Bedard, 1993) within gabbroic mush zones in the magmatic plumbing system below mid-ocean ridges (Sinton & Detrick, 1992). It should be noted that Danyushevsky *et al.* (2003) also presented alternative explanations for the origin of these inclusions, each of which were considered unlikely.

As discussed in detail by Bedard (1993), Bedard *et al.* (2000) and Danyushevsky *et al.* (2003), reactions between plagioclase and primitive melts lead to the formation of aluminous spinel. Thus, unlike commonly considered assimilation processes, dissolution of plagioclase cannot be considered a simple mixing of the primitive melt with the contaminant.

Quantitative modelling of such reactions requires independent constraints on (1) the major and trace element compositions of the primitive melts, contaminant(s) and the reaction products, and (2) the extent of mixing between the reaction products and the primitive melt prior to entrapment, all of which are rarely available. Sample ALV-2384-3 from the Siqueiros Transform Fault is unique in this respect as: (1) the pillow-rim glass of this sample has olivine only on its liquidus (Danyushevsky *et al.*, 2003), and, thus, the composition of primitive melts in equilibrium with high-Fo olivine phenocrysts that contain high-Sr inclusions can be estimated with confidence (see Appendix for calculation details); (2) the sample contains two populations of plagioclase xenocrysts ($An_{85–88}$ and $An_{57–63}$, Danyushevsky *et al.*, 2003), which can be assumed to represent unreacted remnants of mush-zone plagioclase; (3) the high-Sr inclusions also contain aluminous spinel, which has been formed as a result of dissolution reactions.

The results of our modelling are presented in Table 1. High-Sr inclusion S2-OL54-GL, which has the lowest SIE content (Fig. 2a), can be modelled as

$$0{\cdot}64\ \text{Plag} + 0{\cdot}05\ \text{Melt} + 0{\cdot}31\ \text{Oliv} \Rightarrow 0{\cdot}90\ \text{Melt1} + 0{\cdot}10\ \text{Al-Spl} \quad (1)$$

where Plag is plagioclase, Oliv is olivine, Melt is primitive MORB melt, Melt1 is reaction product trapped as inclusion and Spl is spinel. The proportions of phases are from Table 1. The olivine component in this reaction is the host olivine that melted around the trapped plagioclase and melt [see Danyushevsky *et al.* (2003) for detailed discussion]. As can be seen in Table 1, reaction (1) can adequately reproduce all elements in the inclusion S2-OL54-GL, with the exception of Fe, Mg and Cr. This is because the reaction products have re-equilibrated with the host olivine after trapping, as discussed in detail by Danyushvesky *et al.* (2002*c*, 2003).

High-Sr inclusion S1-OL24-GL3, which has the second lowest SIE content (Fig. 2a), cannot be modelled successfully by assuming plagioclase is the only contaminant (unsuccessful models are not presented), and requires dissolution of clinopyroxene to match its composition (Table 1). As sample ALV-2384-3 does not contain clinopyroxene xenocrysts, we have used a composition of clinopyroxene phenocrysts from a Pacific MORB sample 896A-9-1-24 (McNeill & Danyushevsky, 1996), which introduces additional uncertainty in our modelling. Also, the inclusion composition is best modelled assuming the composition of reacting plagioclase is intermediate between the two populations found as

Table 1: Modelling of reactions represented by high-Sr inclusions in sample ALV-2384-3, Siqueiros Transform Fault, East Pacific Rise

No.:	1	2	3	4	5	6	7	8	9	10	11	12	13	14
Inclusion:	S2-OL54-GL; reaction (1)						S1-OL24-GL3; reaction (2)							
Phase:	Plag	Melt	Oliv	Spl	Calc. melt	Melt	Plag	Cpx	Melt	Spl	Oliv	Spl	Calc. melt	Melt
	−	−	−	+	+		−	−	−	−	−	+	+	
Sample no.:	S3-PL21	ALV-2384-3/GL	S2-OL54	S2-OL54-GL-SP		S2-OL54-GL			ALV-2384-3/GL	S1-OL14-SP2	S1-OL24	S1-OL24-GL3-SP		S1-OL24-GL3
SiO_2	45·5	48·7	41·1	0·13	49·2	47·7	48·3	51·3	48·7	0·10	40·8	0·14	48·3	47·7
TiO_2	0·02	0·9	0·0	0·01	0·06	0·04	0·04	0·34	0·9	0·32	0·0	0·05	0·17	0·24
Al_2O_3	34·9	16·2	0·0	64·6	18·5	18·5	33·1	5·2	16·2	37·8	0·0	49·0	17·0	16·7
FeO*	0·3	8·2	9·6	9·4	**2·9**	**8·1**	0·3	4·9	8·2	13·3	9·4	11·5	**3·8**	**8·4**
MnO	0	0·2	0·2	0·1	0·1	0·1	0	0·16	0·2	0·1	0·2	0·1	0·1	0·2
MgO	0·2	11·8	48·8	22·8	**15·1**	**11·1**	0·1	16·9	11·8	18·7	49·3	20·6	**15·8**	**12·0**
CaO	18·0	11·7	0·29	0·06	13·5	13·4	16·0	20·4	11·7	0·05	0·33	0·04	13·5	13·5
Na_2O	1·2	2·2	0	0	0·97	0·97	2·2	0·20	2·2	0	0	0	1·28	1·24
K_2O	0·007	0·024	0	0	0·007	0·003	0·011	0	0·02	0	0	0	0·01	0·01
P_2O_5	0	0·03	0	0	0·00	0·02	0	0	0·03	0	0	0	0·00	0·02
Cr_2O_3	0	0·07	0·05	2·9	**−0·3**	**0·02**	0	0·61	0·07	29·7	0·06	18·5	0·02	0·04
Total	100	100	100	100	100	100	100	100	100	100	100	100	100	100
%	64·0	5·0	31·0	10·0	90·0		46·0	23·0	7·0	2·1	21·9	4·1	95·9	
Ba	0·18	1·23	0	0	0·20	0·15	0·60	0·001	1·23	0	0	0	0·38	0·33
La	0·05	1·10	0	0	0·10	0·05	0·26	0·08	1·10	0	0	0	0·22	0·17
Ce	0·2	4·2	0	0	0·34	0·15	0·6	0·50	4·2	0	0	0	0·73	0·69
Sr	126·4	77·3	0	0	94·2	92·0	221·1	3·87	77·3	0	0	0	113	123
Sm	0·04	2·2	0	0	0·15	0·11	0·07	0·94	2·19	0	0	0	0·42	0·43
Y	0·17	22·6	0·1	0	1·41	1·75	0·34	9·94	22·6	0	0·1	0	**4·2**	**15·7**

1, Plagioclase xenocryst (An_{89}) from sample ALV-2384-3; 2, parental melt of sample ALV-2384-3 calculated from the composition of the pillow-rim glass of this sample (see Appendix); 3, olivine phenocryst from sample ALV-2384-3 that hosts the high-Sr inclusion S2-OL54-GL (Danyushevsky *et al.*, 2003); 4, aluminous spinel within the high-Sr inclusion S2-OL54-GL (Danyushevsky *et al.*, 2003); 5, calculated composition of the melt formed in reaction (1); 6, high-Sr melt inclusion S2-OL54-GL (Danyushevsky *et al.*, 2003); 7, plagioclase An_{80}, whose composition is estimated from the compositions of plagioclase xenocrysts An_{85-88} and An_{57-63} in sample ALV-2384-3; 8, a clinopyroxene phenocryst (Mg-number = 86) from Pacific MORB sample 896A-9-1-24; 9, parental melt of sample ALV-2384-3 calculated from the composition of the pillow-rim glass of this sample (see Appendix); 10, representative spinel from sample ALV-2384-3 (Danyushevsky *et al.*, 2003); 11, olivine phenocryst from sample ALV-2384-3 that hosts the high-Sr inclusion S1-OL24-GL3 (Danyushevsky *et al.*, 2003); 12, aluminous spinel within the high-Sr inclusion S1-OL24-GL3 (Danyushevsky *et al.*, 2003); 13, calculated composition of the melt formed in reaction (2); 14, high-Sr melt inclusion S1-OL24-GL3 (Danyushevsky *et al.*, 2003). Plag, plagioclase; Oliv, olivine; Spl, spinel; Cpx, clinopyroxene; −, phase consumed in the reaction; +, phase formed in the reaction; concentrations of major elements in wt %; concentrations of trace elements in ppm. Values in bold identify elements whose concentrations differ significantly between the analysed and modelled melt composition.

*Total iron as given as FeO.

xenocrysts in sample ALV-2384-3. The relatively high Cr_2O_3 content of the spinel in inclusion S1-OL24-GL3 (Table 1) is best explained by assuming entrapment of a typical MORB spinel together with the reaction products. With the above assumptions, inclusion S1-OL24-GL3 can be modelled as

$$0{\cdot}46\ \text{Plag} + 0{\cdot}23\ \text{Cpx} + 0{\cdot}021\ \text{Cr-Spl} + 0{\cdot}07\ \text{Melt} + 0{\cdot}219\ \text{Oliv} \Rightarrow 0{\cdot}959\ \text{Melt1} + 0{\cdot}041\ \text{Al-Spl} \quad (2)$$

where Cpx is clinopyroxene. The proportions of phases are from Table 1. The olivine component in this reaction is also the host olivine. Differences in FeO* and MgO contents between the modelled and analysed Melt1 compositions are also due to the post-entrapment re-equilibration of the reaction products with the host olivine.

The modelling presented above reproduces the most important compositional features of these high-Sr inclusions, i.e. large positive Sr anomalies, low concentrations of SIE, high CaO and Al_2O_3 contents and low Na_2O contents. It should be noted, however, that reaction (2) cannot reproduce the MIE content of inclusion S1-OL24-GL3 (Y is shown as an example in Table 1), which we do not have an explanation for at the moment. The resolution of this issue is complicated by the uncertainties in the compositions of phases involved in reaction (2), but we believe that this does not invalidate our modelling, as it reproduced the main compositional features of this inclusion.

A successful model for the compositions of the two high-Sr inclusions with SIE contents similar to those of other inclusions in sample ALV-2384-3 (Fig. 2a) should explain the combination of the high Sr contents, relatively 'normal' (i.e. similar to the parental melts of the pillow-rim glasses) major element contents, and high SIE contents. The high Sr contents (i.e. higher than in other high-Sr inclusions from this sample) may reflect dissolution of plagioclase with a higher Sr content, as a result of either a lower An content than the xenocrysts in sample ALV-2384-3, or its crystallization from a melt with a higher Sr content (note that lavas enriched in SIE have been sampled from the Siqueiros Transform in the vicinity of sample ALV-2384-3; Perfit *et al.*, 1996). The high SIE contents of these inclusions may reflect involvement of evolved residual mush-zone melts that can be enriched in SIE. Given these uncertainties in the nature and compositions of the phases involved, we have not attempted modelling of these inclusions.

The high-Sr inclusions from the 43°N MAR sample are likely to represent the products of a reaction similar to reaction (2), as their relatively high CaO and 'normal' Al_2O_3 contents (Fig. 2b; see also Kamenetsky *et al.*, 1998) suggest involvement of clinopyroxene (without clinopyroxene, high CaO is associated with high Al_2O_3 in high-Sr inclusions). Quantitative modelling of these inclusions is hampered by (1) the evolved nature of the pillow-rim glass of this sample (Kamenetsky *et al.*, 1998) and (2) the lack of any information on the compositions of the mineral phases involved; thus it has not been attempted.

Other melt inclusions from samples ALV-2384-3 and 12-7

Danyushevsky *et al.* (2003) have examined in detail major element compositions of inclusions in olivine from sample ALV-2384-3 that do not have Sr anomalies (normal-Sr inclusions; Fig. 2a). Although SIE and MIE contents of normal-Sr inclusions are essentially identical to those of the host lava, their major element contents differ systematically from the estimated parental melt of the pillow-rim glass of the sample (see the Appendix for the details of calculation of the parental melt compositions). Like the high-Sr inclusions from this sample, normal-Sr inclusions also have higher CaO and lower Na_2O and TiO_2 contents than the estimated parental melts (Fig. 2b and c; TiO_2 not shown), although in this case the difference is smaller.

The fact that the average major element composition of the inclusions in high-Fo olivine phenocrysts does not match that of the estimated parental melts for the pillow-rim glass of sample ALV-2384-3 makes it difficult to interpret these inclusions as samples of individual primitive melt fractions, mixing of which leads to the formation of the host lava. The widely accepted idea that individual inclusions in high-Fo olivine phenocrysts represent separate primitive melts within the magmatic system that are well mixed before eruption (Sobolev & Shimizu, 1993) is based on the trace element contents of the inclusions. Indeed, in MORB samples, where inclusions in high-Fo olivine phenocrysts display a large range of SIE contents, most inclusions usually have incompatible element compositions similar to the host lava (e.g. Sobolev, 1996; and the two examples on Fig. 2a). Thus, because of the typically small proportion of anomalous (e.g. high-Sr) inclusions within a particular sample, the average incompatible element content of the melt inclusions is usually similar to that of the host lava. However, major elements are rarely considered in such models.

Lavas that could be derived from primitive melts with major element compositions similar to the normal-Sr inclusions from sample ALV-2384-3 are not known within the Siqueiros transform, or even among MORB worldwide. This raises a question of whether these normal-Sr inclusions are representative of the primitive MORB melts in this area. Moreover, increasing CaO and decreasing Na_2O and TiO_2 contents in the normal-Sr inclusions from sample ALV-2384-3 are accompanied by increasing SIE contents (see Danyushevsky *et al.*, 2003, fig. 8), which would rule out variations in either the degree of melting or the composition of the mantle source

as the reason for the observed range of major element contents in the normal-Sr inclusions [see Danyushevsky *et al.* (2003) for further discussion].

We suggest that compositions of normal-Sr inclusions from sample ALV-2384-3 may also be affected by localized reaction processes, although at this stage we cannot determine the exact mechanism. This interpretation is supported by diffusion of CaO from the normal-Sr melt inclusions into surrounding olivine, as demonstrated by CaO compositional gradients in the host phenocrysts around the normal-Sr melt inclusions (Danyushevsky *et al.*, 2003). Diffusion of CaO out of high-CaO inclusions will be discussed in detail later.

The lack of Sr anomalies suggests that dissolution of plagioclase was not an important process for the origin of normal-Sr inclusions. The high CaO and low Na_2O and TiO_2 contents of the inclusions may suggest dissolution of clinopyroxene; however, this is inconsistent with their 'normal' Al_2O_3 contents (Fig. 2b) and the positive correlation between inclusion CaO and SIE contents. This correlation rules out simple dissolution of any major mineral phase(s) in the gabbroic mush zones as they all have lower SIE concentrations than the melt. However, involvement of small amounts of the residual inter-cumulus melts from the mush zone may produce the observed trends, as such melts are expected to be enriched in SIE. It is also possible that these normal-Sr inclusions represent reaction products that have been extensively (but not completely) mixed with the host magma prior to entrapment.

The evolved nature of the pillow-rim glass of sample 12-7 (Kamenetsky *et al.*, 1998) makes it more difficult to estimate its parental melt composition. As detailed in the Appendix, we considered cases of low-pressure fractionation of olivine and polybaric fractionation of olivine and clinopyroxene (Fig. 2b and c; see also Fig. A1 below). If pillow-rim glasses were formed by low-pressure fractionation of the parental melts, then, similar to the Siqueiros sample, the average composition of normal-Sr inclusions has higher CaO, lower Na_2O and lower TiO_2 contents than the parental melts (Figs 2b and c, and A1). In the case of polybaric fractionation, the average inclusion composition can match the CaO content of the parental melts, but the Na_2O and TiO_2 contents are still lower in the inclusions (Figs 2b and c, and A1). We thus conclude that inclusions in this sample are also unlikely to represent individual primitive melt fractions, mixing of which leads to the formation of the host lava.

The polybaric fractionation of the parental melts can be consistent with the presence of high-magnesian clinopyroxene phenocrysts in sample 12-7 (Kamenetsky *et al.*, 1998). However, we consider this unlikely for two reasons. First, the proportion of olivine to clinopyroxene along the polybaric cotectic shown in Fig. A1b is ~3:1. As clinopyroxene is less dense than olivine, it should be preferentially retained by the ascending melts, and thus we can expect >25% of clinopyroxene in the phenocryst assemblage of the erupted lavas. However, olivine constitutes ~90% of the phenocryst assemblage of the sample (Kamenetsky *et al.*, 1998). Second, the Al_2O_3 content of high-magnesian clinopyroxene phenocrysts is low (3–4 wt %; Kamenetsky *et al.*, 1998), similar to the compositions of magnesian clinopyroxene from 9–10°N MAR that crystallized at ~0·2 GPa (Sobolev *et al.*, 1989), and thus it does not appear to reflect crystallization at high pressure.

Normal-Sr inclusions with the highest CaO contents from sample 12-7 have low Al_2O_3 (Fig. 2b), consistent with dissolution of clinopyroxene. This has been discussed in detail by Kamenetsky *et al.* (1998), who advocated the origin of normal-Sr inclusions via dissolution of clinopyroxene caused by interaction of ascending parental melts with pyroxenite bodies within the mantle. Kamenetsky *et al.* (1998) did not specify whether this interaction occurred on the macro- or micro-scale. Interaction on the macro-scale appears more likely in this scenario, as preservation of micro-scale reaction products as melt inclusions requires high-pressure crystallization of olivine, which we consider unlikely for reasons outlined above. However, interaction on the macro-scale is inconsistent with the difference in major element contents between the average inclusion composition and the estimated compositions of parental melts for sample 12-7 (Figs 2b and c, and A1). Kamenetsky *et al.* (1998) did not discuss this issue in detail, citing the evolved nature of the pillow-rim glass of sample 12-7 (Kamenetsky *et al.*, 1998, p. 121).

Alternatively, interaction with clinopyroxene could occur within the gabbroic mush zone in the lower crust. This scenario places the origin of high- and normal-Sr inclusions from sample 12-7 in a single environment, which is also supported by similar compositions of host olivine for high- and normal-Sr inclusions. Interaction of a primitive melt, saturated in olivine only, with clinopyroxene at crustal pressures leads to formation of high-Cr spinel [see Bedard & Hebert (1998) for a detailed discussion]. This is consistent with the presence of unusually high-Cr spinel inclusions in olivine phenocrysts from sample 12-7 (Kamenetsky *et al.*, 1998). In this scenario, high-magnesian clinopyroxenes in sample 12-7 are xenocrysts that, similar to plagioclase xenocrysts in sample ALV-2384-3, represent unreacted remnants of the mush-zone material. The high-magnesian compositions of these clinopyroxenes may then result from their partial dissolution in the primitive melt. We also favour this scenario as it does not require the presence of clinopyroxenite bodies with the mantle, whose existence beneath the 43°N MAR cannot be demonstrated.

At the same time, we note that the origin of normal-Sr inclusions from sample 12-7 cannot be explained by simple dissolution of clinopyroxene in a single primitive melt, as

there is no correlation between the SEI and CaO contents in the normal-Sr melt inclusions.

ANOMALOUS INCLUSIONS FROM SUBDUCTION-RELATED LAVAS

For the purposes of this section, inclusions from a subduction-related magmatic suite are considered anomalous if their compositions are well outside the range defined by the major element contents of primitive (>6 wt % MgO) rocks from the suite, and 'normal' if they are within that range. Compared with MORB inclusions, anomalous inclusions from subduction-related samples display a much greater range of major element concentrations (Fig. 1). A common feature of anomalous subduction-related inclusions is their high CaO contents, although some anomalously low CaO inclusions also exist.

The major element compositions of anomalous inclusions in high-Fo olivine phenocrysts from primitive subduction-related lavas are shown in Fig. 3. The samples from which inclusion compositions are shown in Fig. 3 cover most of the compositional spectrum of subduction-related magmatism, and were collected from a number of settings worldwide (see Fig. 3 caption for details). Inclusion compositions are compared with the field of published primitive subduction-related volcanic rocks from the same locations (see Fig. 3 caption for details). It should be noted that, for clarity, 'normal' inclusions from subduction-related lavas are not plotted in Fig. 3.

Anomalous inclusions from all subduction-related samples that are characterized by increasing TiO_2 with increasing CaO form the 'high-TiO_2' trend in Fig. 3 (red triangles). In all other plots, most of the high-TiO_2 inclusions overlap with those characterized by decreasing Al_2O_3 with increasing CaO (the 'low-Al_2O_3' trend; yellow circles). However, some of the high-TiO_2 inclusions also have high Al_2O_3 contents. Other inclusions characterized by increasing Al_2O_3 with increasing CaO but 'normal' TiO_2 contents define the 'high-Al_2O_3' trend (green squares). In other plots, the 'high-Al_2O_3' trend overlaps with the 'low-Al_2O_3' trend. We have also identified a high-CaO, high-SiO_2 trend ('high-SiO_2' trend; maroon stars), a low-CaO, high-SiO_2 trend (blue circles), and a low-CaO, low-SiO_2 trend (purple diamonds), all of which are distinct in all plots on Fig. 3.

The compositions of melt inclusions at the extremes of each trend (Table 3) do not resemble any primitive magma compositions either sampled in subduction-related settings or produced experimentally [see also the discussion by Kogiso & Hirschmann (2001)].

In general, each trend includes inclusions from different samples from different localities, and inclusions from a single sample can be present in different trends. For example, inclusions from sample EL-9 (Tavua shoshonitic volcanic centre in Fiji; this study) plot within the low-CaO, high-SiO_2 trend, the low-CaO, low-SiO_2 trend, and the low-Al_2O_3 trend with both high- and normal-P_2O_5 contents, and this sample also has numerous 'normal' inclusions. Compositions of representative inclusions from this sample are presented in Tables 2 and 3.

In some samples, all inclusions in high-Fo olivine phenocrysts (Fo >85) have anomalous compositions. For example, inclusions in high-Fo olivines from Tavua sample EL-10 (Table 2) have anomalously high CaO contents (Fig. 4), plotting along the high-TiO_2 and low-Al_2O_3 trends in Fig. 3. Inclusions in less forsteritic olivine phenocrysts ($Fo_{80–79}$) from this sample are similar to the compositions of evolved lavas of the Tavua suite (MgO <4 wt %; Fig. 4). Similar observations have been made elsewhere (e.g. Schiano *et al.*, 2000).

Samples EL-9 and EL-10 have been collected in close proximity to each other from the same volcano. These samples have very similar major element compositions (Table 2) and the same range of olivine phenocryst compositions (Fig. 4). However, samples EL-9 and EL-10 differ in the size and abundance of melt inclusions in high-Fo olivines. In EL-10, where all inclusions have anomalous compositions, melt inclusions are large (up to 200 μm; Fig. 5a) and numerous, whereas in EL-9, where a large proportion of inclusions have 'normal' compositions, inclusions are rare and small (<50 μm; Fig. 5b).

Sample D2-1 from the Hunter Ridge also has both normal and anomalous inclusions in high-Fo olivine phenocrysts (Tables 2 and 3). However, unlike EL-9, this sample contains numerous large inclusions (Fig. 5c). Anomalous inclusions in this sample plot at the extreme end of the 'high-SiO_2' trend (Fig. 3). The compositions of these inclusions are highly depleted in Al_2O_3, TiO_2, Na_2O and K_2O, and, in many respects, they resemble the composition of clinopyroxene. Although these compositions clearly reflect melting of clinopyroxene, it is important to note that they cannot represent complete melting of an accidentally trapped clinopyroxene during experimental reheating. This is demonstrated in Table 1 by modelling the mixing of a normal inclusion from sample D2-1 with a high-magnesian clinopyroxene from this sample. Although such mixing can reproduce a number of the compositional features of the anomalous inclusions, it results in a significantly lower FeO content. The modelling also indicates that the proportion of clinopyroxene in the mix should be ~75 wt % to match the Al_2O_3 and Na_2O contents of the anomalous inclusion. This would require the presence of a large (~50 vol. %), easily identifiable clinopyroxene crystal in the inclusion, which is clearly not the case as this inclusion has been recrystallized to a fine-grained aggregate during natural cooling (Fig. 5d), typical for all inclusions in this sample

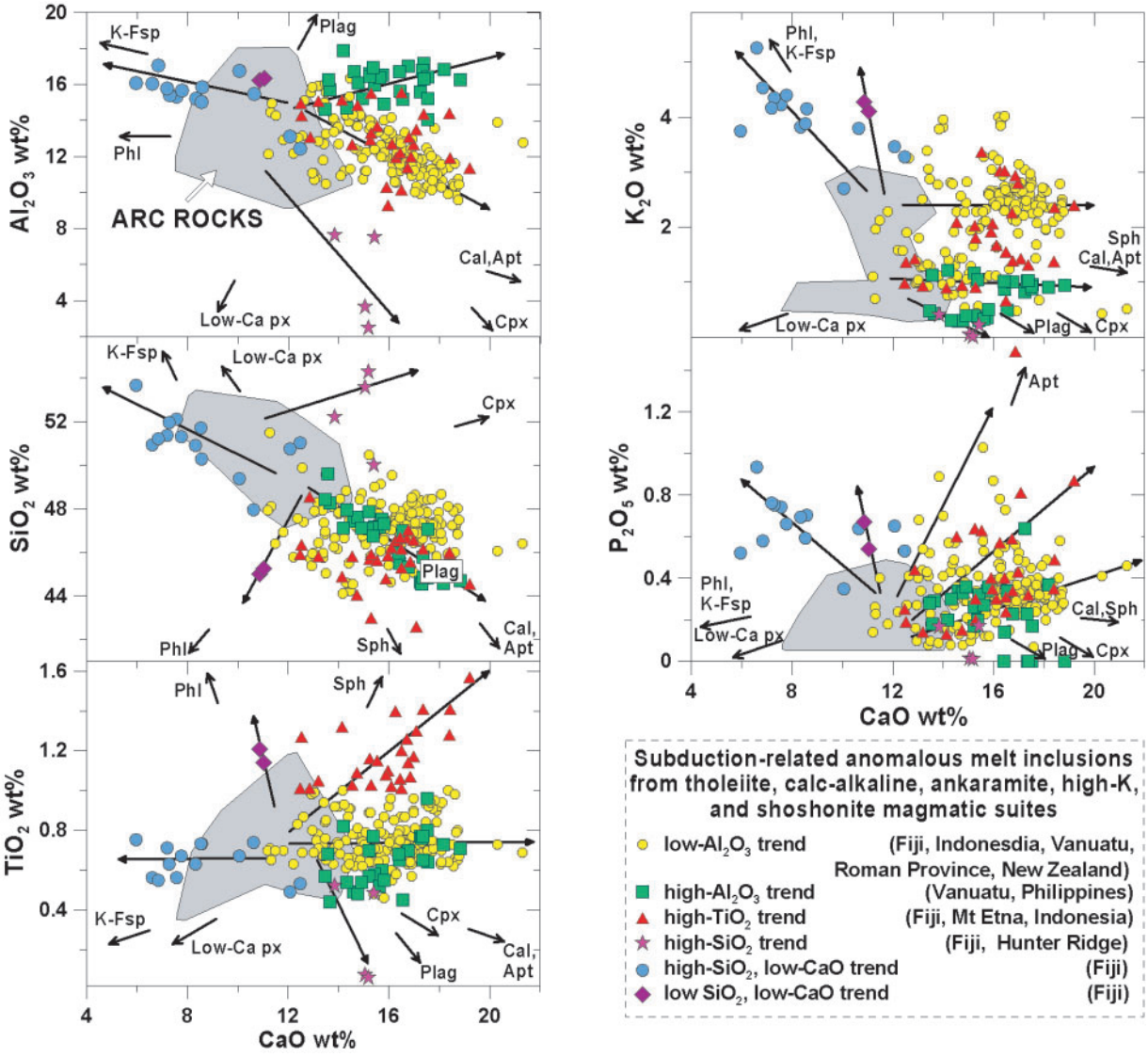

Fig. 3. Compositions of anomalous melt inclusions in high-Fo olivine from primitive subduction-related samples. Our data from Fiji and the Hunter Ridge are complemented by inclusion compositions from Kamenetsky & Clocchiatti (1996), Della-Pasqua (1997), Della-Pasqua & Varne (1997), Gioncada *et al.* (1998), Sisson & Bronto (1998), Metrich *et al.* (1999) and Schiano *et al.* (2000). The dataset includes primitive samples from tholeiitic, calc-alkaline, ankaramitic, high-K, and shoshonitic magmatic suites from New Zealand, Fiji, the Hunter Ridge, Vanuatu, Indonesia, the Philippines, the Roman Province and Mt. Etna. The inclusions are grouped by their chemical affinities. Green squares, high-Al_2O_3, high-CaO trend (inclusions from Vanuatu and the Philippines); red triangles, high-TiO_2, high-CaO trend (inclusions from Fiji, Mt Etna and Indonesia); blue circles, high-SiO_2, low-CaO trend (inclusions from Fiji); maroon stars, high-SiO_2, high-CaO trend (inclusions from Fiji and the Hunter Ridge); purple diamonds, low-SiO_2, low-CaO trend (inclusions from Fiji); yellow circles, low-Al_2O_3, high-CaO trend (inclusions from Fiji, Indonesia, Vanuatu, the Roman Province and New Zealand). It should be noted that some trends overlap on some plots. Arrows point to approximate positions of 'average' compositions of calcic plagioclase (Plag), clinopyroxene (Cpx), apatite (Apt), calcite (Cal), titanite (Sph), low-Ca pyroxene (low-Ca px), K-feldspar (K-fsp) and phlogopite (Phl). (See text for discussion.)

(Fig. 5c). This indicates that these inclusions had anomalous compositions prior to experimental reheating. The high FeO content of the inclusions is probably explained by post-entrapment re-equilibration with the host phenocryst (Danyushevsky *et al.*, 2000*a*, 2003).

Extreme anomalous inclusion compositions, such as those from sample D2-1, are rarely found. Such compositions require entrapment prior to any significant mixing of the dissolved contaminant(s) with the host magma, and thus they are significantly easier to interpret. In most cases, anomalous inclusions represent compositions that have been variably mixed with the host magma prior to entrapment. Such mixing masks the initial characteristics of the contaminant(s) and makes it significantly more difficult to understand the origin of anomalous inclusions.

Table 2: Examples of normal and anomalous melt inclusions from samples EL-9 (Fijian shoshonites) and D2-1 (Hunter Ridge tholeiite)

Location:	Fiji, shoshonites						Hunter Ridge, tholeiites				
Sample type:	WR	WR	WR	MI	MI	MI	WR	MI	MI	Cpx	Calc.
Inclusion type:				normal	anomalous	anomalous		normal	anomalous		
Trend in Fig. 3:					low-CaO, high-SiO_2	low-Al_2O_3, low-P_2O_5			high-SiO_2		
Sample no.:	EL8	EL9	EL10	EL9/OL-4/222x	EL9/OL-5/38	EL9/OL-4/269	D2-1	D2-1/B1-OL217	D2-1/B10-OL24	D2-1/B10-CP41	
SiO_2	49·71	49·69	49·68	47·66	49·4	47·3	51·86	54·00	53·57	53·71	53·78
TiO_2	0·57	0·57	0·57	0·64	0·67	0·65	0·36	0·29	0·07	0·10	0·15
Al_2O_3	12·37	12·67	12·4	15·63	16·75	14·24	11·53	11·12	3·65	1·37	3·81
FeO*	9·63	9·65	9·56	8·79	9·24	8·86	7·36	8·44	11·49	3·95	5·08
MnO	0·21	0·2	0·21	0·08	0·12	0·13	0·15	0·12	0·25	0·13	0·13
MgO	11·31	11·02	10·97	9·56	7·96	8·77	16·28	13·64	15·19	18·02	16·92
CaO	12·14	11·77	12·26	12·17	10·06	14·87	7·74	9·86	15·05	21·94	18·92
Na_2O	2·2	2·12	2·17	2·52	2·7	2·56	2·27	2·17	0·55	0·18	0·68
K_2O	1·5	1·97	1·83	2·44	2·7	2·27	0·51	0·24	0·05	—	0·06
P_2O5	0·35	0·35	0·35	0·33	0·35	0·29	0·06	0·05	0·02	—	0·01
Cr_2O_3	—	—	—	0·17	0·05	0·04	0·21	0·06	0·11	0·60	0·46
Total	100	100	100	100	100	100	100	100	100	100	100
Fo host	—	—	—	90·83	88·28	90·17	—	89·8	90·0	89·0†	—

WR, whole-rock composition; MI, melt inclusion composition; Cpx, composition of high-magnesian clinopyroxene from sample D2-1; Calc., modelled composition of the anomalous inclusion D2-1/B10-OL24, calculated as mixture of 75% clinopyroxene and 25% of the normal inclusion D2-1/B1-OL217. Fo host, composition of host olivine phenocrysts (mol %).
*All Fe as given as FeO.
†Mg-number of clinopyroxene; all inclusions have been reheated to remelt the daughter crystals, as described in the text, and quenched to glass; all compositions are normalized to 100% anhydrous.

Table 3: Compositions of melt inclusions at the extremes of each trend in Fig. 3

	1	2	3	4	5	6	7
Location:	Fiji	Hunter Ridge	Fiji	Philippines	Fiji	Indonesia	Fiji
Magma type:	shoshonite	tholeiite	shoshonite	calc-alkaline	shoshonite	ankaramite	shoshonite
Trend in Fig. 3:	low-CaO, high-SiO_2	high-SiO_2	low-CaO, low-SiO_2	high-Al_2O_3	high-TiO_2	low-Al_2O_3, low-P_2O_5	low-Al_2O_3, high-P_2O_5
Sample no.:	VT-3/OL-1/24	D2-1/B1-OL109	EL9/OL-3/133	B45/53	EL10/OL-2/4 m-2	DP97-48001/OL84	EL9/OL-5/542
SiO_2	53·68	54·31	45·02	44·57	45·93	44·88	47·76
TiO_2	0·75	0·06	1·21	0·73	1·41	0·92	0·64
Al_2O_3	16·07	2·49	16·21	16·83	11·92	12·21	13·39
FeO*	10·02	11·09	8·83	7·34	9·24	10·29	9·21
MnO	0·17	0·22	0·09	0·12	0·12	0·17	0·11
MgO	6·10	16·22	9·20	8·22	8·38	11·37	7·98
CaO	5·96	15·18	10·86	18·17	18·43	17·58	15·58
Na_2O	2·93	0·28	3·56	2·73	1·65	1·55	2·11
K_2O	3·74	0·01	4·28	0·91	2·36	0·97	2·09
P_2O_5	0·52	0·01	0·67	0·37	0·49	0·07	1·03
Cr_2O_3	0·05	0·14	0·09	—	0·07	—	0·11
Total	100	100	100	100	100	100	100
Fo host	83·8	90·5	91·4	88·6	89·6	90·2	88·4

Fo host, composition of host olivine phenocrysts (mol %); all inclusions have been reheated to remelt the daughter crystals, as described in the text, and quenched to glass; all compositions are normalized to 100% anhydrous; analyses 4 and 6 are from Metrich *et al*. (1999) and Della-Pasqua (1997), respectively.
*All Fe given as FeO.

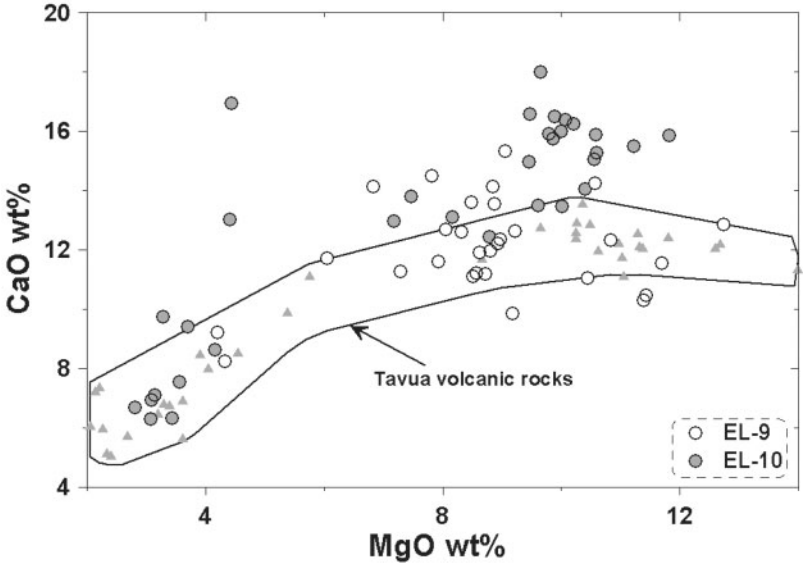

Fig. 4. CaO vs MgO (wt %) contents of melt inclusions in olivine ($Fo_{78–91}$) phenocrysts from samples EL-9 (open circles) and EL-10 (filled circles) from the Tavua shoshonitic volcanic centre in Fiji. Compositions of the Tavua volcanic rocks are shown by grey triangles. The difference in CaO contents of the high-MgO inclusions between the two samples should be noted. (See text for discussion.)

Inclusions with anomalously low-CaO contents represent examples where clinopyroxene has not affected their compositions. Such inclusions are best represented by sample VT-3 from another Fijian shoshonitic centre (Vatu-i-Cake island). The VT-3 inclusions define a trend of increasing SiO_2, Al_2O_3, K_2O and P_2O_5 contents with decreasing CaO (the low-CaO, high-SiO_2 trend, Fig. 3), whereas TiO_2 and Na_2O contents remain

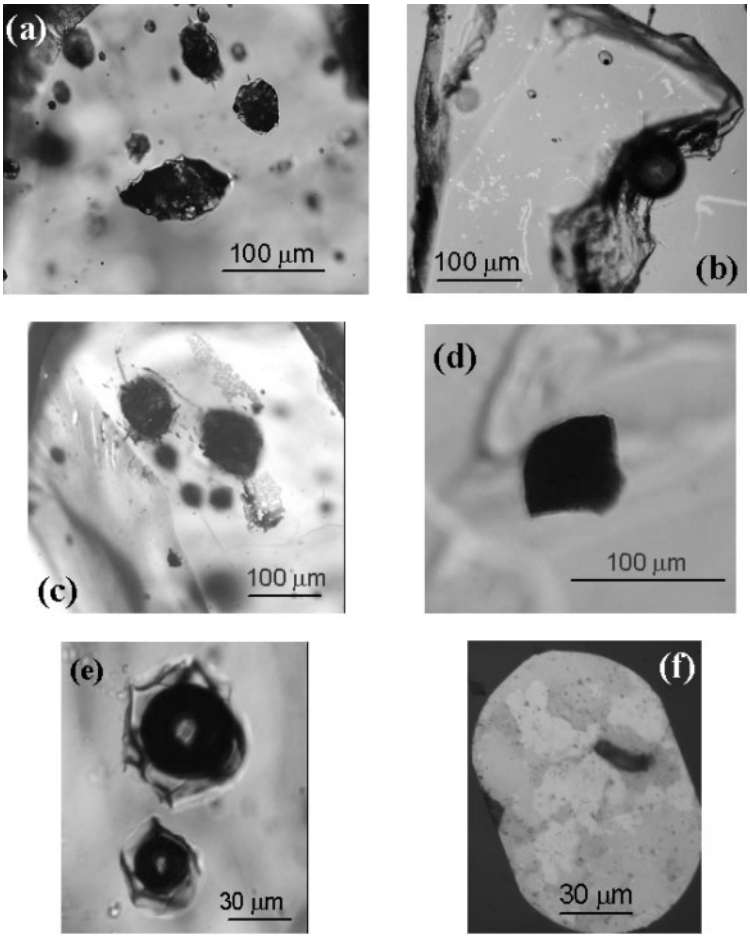

Fig. 5. (a) Recrystallized melt inclusions in an olivine phenocryst from sample EL-10, Fiji. The numerous large inclusions should be noted. (b) Naturally quenched glassy melt inclusions in an olivine phenocryst from sample EL-9, Fiji. The rare small inclusions should be noted. (c) Recrystallized melt inclusions in olivine phenocryst from sample D2-1, the Hunter Ridge, SW Pacific. The numerous large inclusions should be noted. (d) Recrystallized anomalous inclusion D2-1/B10-OL24 in olivine $Fo_{90\cdot0}$ (sample D2-1, the Hunter Ridge, SW Pacific). (e) Primary fluid inclusion in olivine phenocryst S2-OL98 ($Fo_{90\cdot3}$) from sample ALV-2384-3, Siqueiros Transform Fault, EPR. (f) Primary sulphide inclusion in olivine phenocryst S1-OL41 ($Fo_{90\cdot5}$) from sample ALV-2384-3, Siqueiros Transform Fault, EPR.

constant. Some inclusions from Tavua shoshonites (Table 2) also plot along this trend. This trend can be reproduced by the assimilation of a K-feldspar–biotite–apatite assemblage by a primitive shoshonitic magma.

Like Tavua, Vatu-i-Cake represents the subaerial expression of a large Pliocene (3·84 Ma; Whelan *et al.*, 1985) volcanic complex that lies within the Fijian arc-crust, of which a substantial component is likely to be monzonitic (intrusive equivalent of evolved shoshonite) (Gill & Whelan, 1989; Setterfield *et al.*, 1991; D. Carroll, personal communication, 2002). As K-feldspar, biotite and apatite are all essential phases in monzonites, the likely origin of the low-CaO, high-SiO_2 trend at both volcanic centres is from the interaction between primitive shoshonitic magma and a pre-existing monzonitic crust or semi-solidified mush zone.

Figure 3 shows arrows to several mineral phases that may be expected to occur within the mush zones of the magmatic plumbing systems in subduction-related settings. Each of the trends defined by anomalous inclusions can be explained by contamination of a primitive subduction-related magma with a combination of these phases. As discussed in the previous section, this type of assimilation does not always represent simple admixing of contaminants to the primitive magma, as some of the phases may melt incongruently. Lack of detailed knowledge of the dissolution reactions makes it difficult to quantitatively model the compositions of the anomalous inclusions. This modelling is further complicated by post-entrapment diffusive re-equilibration of the inclusions with their hosts, which resets the Fe/Mg values of the inclusions (Danyushevsky *et al.* 2000*a*).

DISCUSSION

The presence of anomalously high-CaO melt inclusions in high-Fo olivine phenocrysts from various magmatic suites has been emphasized previously (e.g. Kamenetsky & Clocchiatti, 1996; Kamenetsky *et al.*, 1997, 1998; Metrich *et al.*, 1999). On the basis of the compositions of high-Ca inclusions from subduction-related settings, Schiano *et al.* (2000) have proposed the existence of a distinct type of primitive, low-SiO_2, high-CaO magma in island-arc settings. Schiano *et al.* (2000) suggested that such magmas form during melting of clinopyroxene-rich lithologies in the shallow mantle wedge and/or lower arc crust. Because, in samples described by Schiano *et al.* (2000) all inclusions in olivine phenocrysts with Fo >85 have high CaO contents whereas inclusions in olivine phenocrysts with lower Fo contents have 'normal' arc compositions (this is similar to sample EL-10 from Fiji described above), those workers further suggested that the compositional variations among high-Ca inclusions reflect mixing between the high-CaO magma and the most primitive 'normal' arc melts trapped in olivine Fo_{85}.

Regardless of whether low-SiO_2, high-CaO compositions can be produced during melting of a clinopyroxene-rich source [see discussion by Kogiso & Hirschmann (2001)], a number of observations make this explanation for the origin of the anomalous high-Ca inclusions unlikely.

Most importantly, in subduction-related samples, anomalous inclusions with very different compositions can coexist in one sample (see examples above). Moreover, in compositionally similar samples collected from a single volcano, melt inclusions can display a range of anomalous compositions. A good example of this occurs at the Tavua shoshonitic volcanic centre in Fiji. Samples EL-8, EL-9 and EL-10 all have similar major element compositions (Table 2) and the same range of Fo contents of olivine phenocrysts (Fig. 4). Sample EL-8 has three types of high-CaO inclusions within the 'high TiO_2' and 'low-Al_2O_3' trends in Fig. 3 (the 'low-Al_2O_3' inclusions have both high and low P_2O_5 contents), and this sample also has high-SiO_2, low-CaO inclusions. Sample EL-9 has 'normal' inclusions, two types of low-Ca inclusions (with high and low SiO_2) and high-CaO, low-Al_2O_3 inclusions with both high and low P_2O_5 contents. Sample EL-10 has high-CaO inclusions only, which belong to the high-TiO_2 and low-Al_2O_3 trends (Fig. 3). It is unlikely that five different primitive magmas, all with vastly different anomalous compositions, have simultaneously existed under this volcano, and that none of these magmas has erupted or, at least, significantly affected (by mixing) the compositions of the erupted lavas (all of which are typical primitive shoshonites; Table 2).

The high-CaO, low-Al_2O_3 inclusions from Tavua samples are very similar to the high-CaO, low-Al_2O_3 inclusions from Vanuatu, Indonesia, New Zealand and the Roman Volcanic Province in Italy (references are given in the caption to Fig. 3); although the samples from the literature have not been studied in as much detail as the Fijian shoshonites, it is likely that all such inclusions have similar origin.

Gaetani *et al.* (2002) have suggested that the anomalously high CaO contents of inclusions in high-Fo olivine may result from CaO diffusion into the inclusions from their host phenocrysts, caused by an increase in the activity of CaO in the magma around the host phenocryst. However, this mechanism is unlikely to be responsible for the anomalous high-CaO inclusions in our samples, as compositional profiles through olivine adjacent to the high-CaO inclusions indicate that CaO diffuses out of them, i.e. there is a decrease in the CaO content of olivine away from the inclusions. This is demonstrated in Fig. 6, which presents compositional profiles through livine around two inclusions from sample D2-1, for which compositions are presented in Tables 2 and 3. There is a clear gradient in CaO content in the olivine around anomalous inclusion D2-1/B1-OL109, whereas no measurable gradient is observed around 'normal' inclusion D2-1/B1-OL217. As discussed in detail by Danyushevsky *et al.* (2003), diffusion of CaO out of anomalous inclusions is an indication that the trapped composition had a CaO content that was too high to be in equilibrium with the host at the moment of entrapment.

In many samples with anomalous primitive inclusions described above, either from MORB or subduction-related suites, none of the inclusions in high-Fo phenocrysts have 'normal' compositions. High-Fo olivine phenocrysts in these samples are generally characterized by large (100–200 μm inclusions are common), abundant melt inclusions. The occurrence of numerous large inclusions probably indicates fast crystallization rates of the high-Fo phenocrysts (Roedder, 1984).

Fast crystallization rates can be caused by a fast cooling rate; however, it is important to note that high-Fo olivine phenocrysts most probably crystallize within the plumbing system prior to eruption [see discussion by Danyushevsky *et al.* (2002*c*)]. Considering the origin of high-Fo olivine-phyric volcanic rocks in detail, Danyushevsky *et al.* (2002c) have advocated a magmatic plumbing system (after Sinton & Detrick, 1992; Marsh, 1995, 1998), which involves magma passing through a sequence of interconnected chambers with well-developed mush columns (Fig. 7). The mush columns contain crystals and residual melts left behind by passing magma batches that fractionate *en route* to eruption, and in general, the mineral phases coexisting in the mush zones will often be derived from variably evolved magmas (Sinton & Detrick, 1992; Davidson & Tepley, 1997; Marsh, 1998; Gamble *et al.*, 1999; Cole *et al.*, 2001). The actual temperature and composition of the mush zone

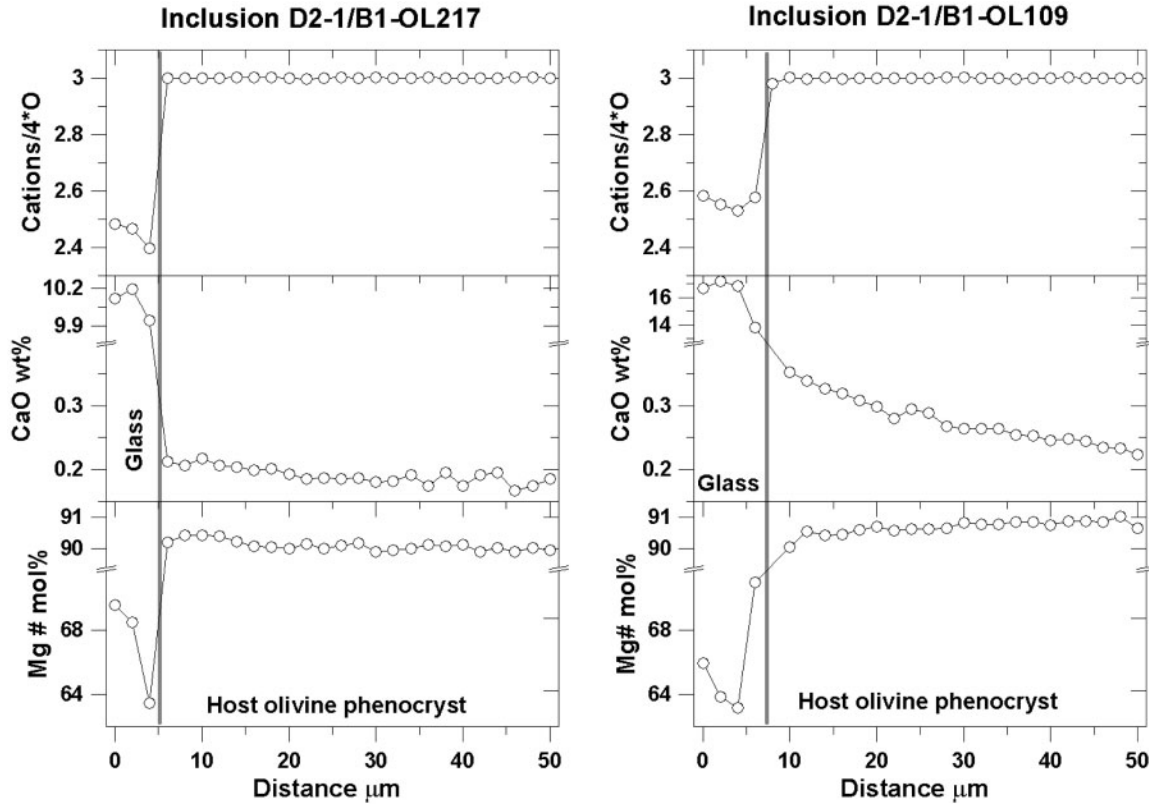

Fig. 6. Compositional profiles in olivine phenocrysts around two melt inclusion from sample D2-1 from the Hunter Ridge. The compositions of these inclusions are given in Tables 2 and 3. Inclusion D2-1/B1-OL217 is normal, whereas inclusion D2-1/B1-OL109 is anomalous, representing the extreme of the 'high-SiO_2' trend in Fig. 3. Profiles were analysed on two sides of the inclusions and are symmetrical. Mg-number = 100Mg/(Mg + Fe). Position of the glass–olivine boundary (thick grey line) is determined using stoichiometry (cations per four oxygens; Danyushevsky *et al.*, 2000*a*). Analyses at the boundary are affected by the analytical overlap between glass and olivine. The increasing CaO contents in olivine around the anomalous inclusion should be noted. (See text for discussion.)

will generally depend on the rate of supply of primitive magma into the plumbing system. However, in most cases the extent of mush-column fractionation is large, as indicated by the eruption temperatures and groundmass compositions of the erupted olivine-phyric lavas [see the detailed discussion by Danyushevsky *et al.* (2002*c*)]. Consequently, the mush zones are in general significantly cooler than the primitive magma, and therefore a significant portion of the crystal mass is not in equilibrium with the primitive magma.

Within the plumbing system, the fastest cooling rates of the primitive magma are expected at its margins (Huppert & Sparks, 1980), where it is in contact with the wall rocks and/or pre-existing semi-solidified mush zones (depending on the specific environment). This localized cooling of the primitive melt will be accompanied by partial dissolution of the mush-zone phases that are not in equilibrium with the primitive melt, and mixing of the reaction products with the primitive magma [dissolution–reaction–mixing (DRM) processes].

In such environments the contaminant is often comagmatic and geologically contemporaneous; that is, it represents phases formed during fractionation of earlier batches of the same magma type. As a result, although they create large localized heterogeneities in major and trace element compositions, the DRM processes do not necessarily lead to obvious isotopic anomalies.

Also unlike commonly considered assimilation processes, the DRM processes may involve incongruent melting and formation of new phases [e.g. a case with aluminous spinel described above; also see Bedard & Hebert (1998)]. Quantitative modelling of the DRM processes thus requires experimental investigation of the reactions between a specific primitive melt and a specific contaminant.

Rapid cooling within these reaction zones should facilitate localized rapid crystallization of high-Fo olivines from the primitive magma (Fig. 7), leading to entrapment of numerous large inclusions (Fig. 5a). The compositions of such inclusions are likely to record the DRM processes in progress, which leads to the anomalous major and/or trace element compositions of inclusions.

The trends, defined by anomalous inclusions in subduction-related magmas in Fig. 3, probably represent

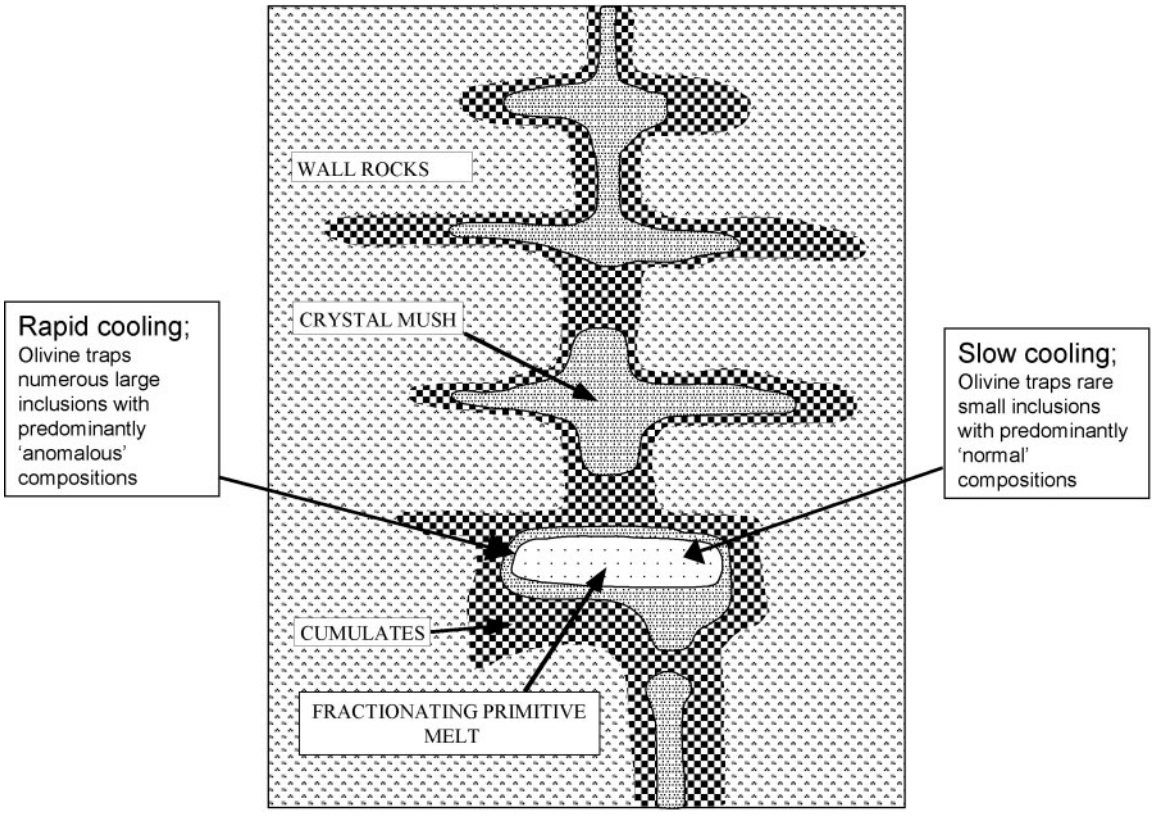

Fig. 7. Schematic illustration of a magmatic plumbing system dominated by well-developed mush zones (after Marsh, 1995, 1998). A primitive magma experiences rapid localized cooling at its margins, where it is in contact with the wall rocks and/or pre-existing semi-solidified mush zones. This is accompanied by partial melting of the mush-zone phases and mixing of the reaction products with the primitive magma. Rapid cooling within these reaction zones facilitates localized rapid crystallization of high-Fo olivines, leading to entrapment of numerous large inclusions with predominantly anomalous compositions. Inside the magma body, away from the reaction zones, slower cooling rates do not favour trapping of inclusions, and thus 'normal' inclusions are much less common and small. (See text for discussion.)

variable extents of mixing between the reaction products and the primitive magma prior to entrapment by the olivine phenocrysts. The interpretation of the mechanisms leading to the formation of the anomalous inclusion compositions would be significantly aided by the occurrence of inclusions whose compositions are minimally affected by pre-entrapment mixing. However, such inclusions are extremely rare (the only two examples known to us are inclusions S2-OL54-GL from sample ALV-2384-3 from the Siqueiros Transform, which records dissolution of plagioclase, and B1-OL109 from sample D2-1 from the Hunter Ridge, which records dissolution of clinopyroxene), which has complicated the identification of specific DRM reactions and has led to a number of alternative explanations for the origin of anomalous inclusions (see discussion above).

Inside the magma body, away from the reaction zones, slower cooling rates do not favour trapping of inclusions (Fig. 7), thus 'normal' inclusions are much less common and small (Fig. 5b). Thus we suggest that the difference between Fijian shoshonite samples EL-9 and EL-10, which have been described in detail above, are due to sample EL-9 containing olivine phenocrysts that crystallized mainly inside the magma body, whereas olivine phenocrysts in sample EL-10 crystallized at the margins of the magma body.

We consider that the population of melt inclusions in high-Fo olivine phenocrysts is naturally biased towards anomalous compositions when crystallization occurs in response to rapid cooling within the magmatic plumbing system. This natural bias is further advanced by our preference for selecting samples for analysis with numerous large melt inclusions, because of their ease of study and suitability for a range of microanalytical techniques.

An alternative cause for fast crystallization rates of high-Fo olivine is the loss of H_2O during degassing of a primitive magma at shallow levels, as a result of the well-known effect of H_2O on depressing melt crystallization temperature. This can occur in tectonic settings where primary magmas either have high H_2O contents or are able to ascend to the surface bypassing well-developed magmatic plumbing systems. Crystallization accompanied by degassing has been documented for

high-Ca boninites from the northern termination of the Tonga Arc (Danyushevsky *et al.*, 1995) and komatiites from Belingwe, Zimbabwe (Danyushevsky *et al.*, 2002*a*). In both cases high-Fo olivines contain numerous large inclusions that all have 'normal' compositions. However, crystallization during degassing does not preclude the occurrence of DRM processes. For example, high-Fo olivines from sample D2-1 from the Hunter Ridge have numerous large 'normal' inclusions, but anomalous inclusions are also common. Crystallization of high-Fo olivine from this sample is interpreted to have been accompanied by degassing of an H_2O-rich fluid, as indicated by the presence of primary H_2O-rich fluid inclusions (Durance-Sie *et al.*, in preparation).

DRM processes should have the largest impact on the compositions of melt inclusions trapped by olivine phenocrysts that crystallize early from hot primitive mafic magmas. In contrast, the more 'evolved' (less forsteritic) olivine phenocrysts crystallize from melts that are comparatively cooler, and, therefore, have less reaction potential because of their lower temperature and reduced compositional contrast with the mush-zone phases. This can explain why anomalous inclusions are preferentially found in high-Fo olivine phenocrysts relative to evolved phenocrysts.

The proposed mechanism for the origin of anomalous inclusions is consistent with the wider range of anomalous major element concentrations in inclusions from primitive subduction-related lavas relative to MORB. Primitive subduction-related magmas undergo more substantial fractionation than MORB (e.g. andesites and more evolved lavas are common in subduction-related settings, whereas erupted MOR melts are largely basaltic). Generally, this is because subduction-related magmas have higher H_2O contents and occur in settings with thicker crust. The greater extent of fractionation of the subduction-related magmas generally leads to a larger variety of mineral types in the mush zones within the plumbing systems. Thus, in the subduction-related settings there are generally greater temperature differences and compositional disequilibrium between the primitive melts and the mush-zone assemblage, both facilitating the DRM processes.

A possible role for DRM processes in the origin of some anomalous inclusions has been also suggested by Bedard *et al.* (2000). Considering in detail the structure and composition of the lower crust of the Bay of Islands Ophiolite, Newfoundland, they suggested that diverse populations of melt inclusions in MORB olivine phenocrysts can be explained by crystallization of these olivines in a contaminated boundary layer where the primitive magma interacts with the walls of an intracrustal conduit; the diverse inclusion populations represent incomplete mixing in these contaminated boundary layers.

Additional considerations of the effects of the DRM processes on MORB melt inclusions

As a result of DRM processes, the compositions of inclusions that contain the reaction products are depleted in elements that are incompatible in the solid phases involved (see Table 1 for some examples). This is usually more pronounced in MORB than in subduction-related inclusions, as the geochemical characteristics of the latter are more diverse because of the involvement of slab-derived component(s). In inclusions with compositions affected by the DRM processes, elements that are similarly incompatible in the dissolution reactions form well-defined trends in element–element variation diagrams, which pass through the composition of the parental melt of the sample and the origin (Fig. 8). It should be noted that the 'apparent' relative incompatibilities recorded by these trends differ significantly from those during mantle melting. For example, in sample ALV-2384-3, the high-Sr, SIE-depleted inclusions whose compositions reflect dissolution of plagioclase (± clinopyroxene), display apparent incompatibility of Zr that is the same as that of Ce and Sm. The observed relationship cannot be produced during mantle melting, where Ce is significantly more incompatible than Sm (e.g. Sun & McDonough, 1989), but is consistent with DRM reactions dominated by plagioclase, as all three elements are strongly incompatible with this mineral. As minerals involved in the reactions considered here do not contain volatiles, the anomalous inclusions from sample ALV-2384-3 that have low concentrations of SIE are also volatile undersaturated (S is shown as an example in Fig. 8).

This issue is emphasized here because the compositions of the inclusions from the Siqueiros samples, which we consider to reflect variable extents of DRM processes, have been used by Sobolev & Hofmann (1999) and Saal *et al.* (2002) to infer relative compatibility of volatile elements (S and CO_2) during mantle melting. Both studies used inclusions from samples collected from dive ALV-2384, including sample ALV-2384-3 considered in detail here and by Danyushevsky *et al.* (2003). Although inclusions affected by the dissolution reactions are indeed undersaturated in volatiles, their compositions cannot be used to infer magma generation conditions. We also suggest that the parental melts for sample ALV-2384-3 have been saturated in both CO_2-rich fluid and sulphide melt at the depths of crystallization, as some olivine phenocrysts contain fluid and sulphide inclusions (Fig. 5e and f).

The effects of DRM processes on the compositions of erupted lavas

Despite having a significant impact on the compositions of melt inclusions in high-Fo olivines, DRM

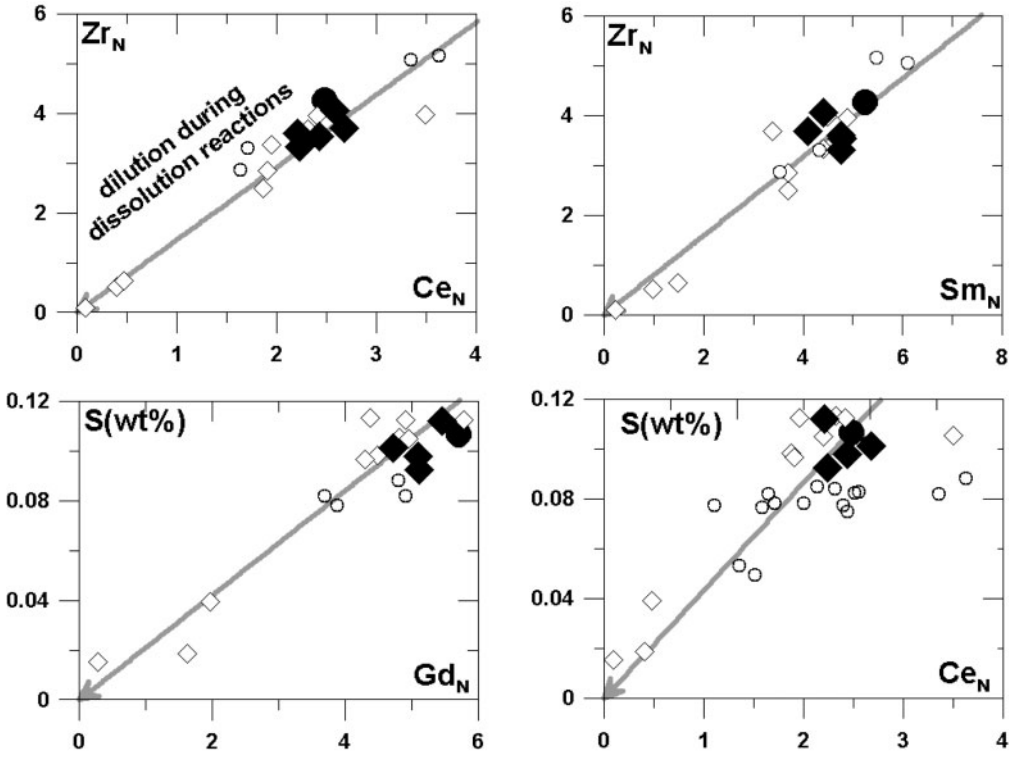

Fig. 8. Compositions of melt inclusions in high-Fo olivine phenocrysts from MORB from the Siqueiros Transform Fault, EPR. Open diamond, normal-Sr inclusions from this study; large filled diamonds, high-Sr inclusions from this study; open circles, compositions from Saal *et al.* (2002); large filled circles, compositions of pillow-rim glass from sample ALV-2384-3 (Danyushevsky *et al.*, 2003). To account for effects of fractionation, all compositions are recalculated as described in the Appendix. All elements except S are normalized to the primitive mantle of Sun & McDonough (1989). Grey arrows show best-fit lines that pass through the origin. The systematic difference in S contents between the datasets of Saal *et al.* (2002) and Danyushevsky *et al.* (2003) is due to employment of different analytical techniques, as demonstrated by analysed S contents in pillow-rim glass ALV-2384-3: 1090 ppm found by Danyushevsky *et al.* (2003) vs 935 ppm found by Saal *et al.* (2002). (See text for discussion.)

processes are generally less important for the main volume of melt within the magmatic plumbing system, as they are not recorded in the compositions of erupted lavas shown in Figs 2 and 3. However, in some cases the effects of DRM processes can also be identified in the erupted lavas. Figure 9 presents compositions of melt inclusions in olivine compared with the host lavas from primitive Icelandic tholeiites (Hengill swarm, Gurenko & Chaussidon, 1995). The trace element patterns of the SIE-depleted inclusions from these samples are similar to the high-Sr, SIE-depleted inclusions from MORB samples ALV-2384-3 and 12-7 (Fig. 2). However, unlike those two examples, the host Icelandic lava also has a positive Sr anomaly [other high-Sr examples of primitive Icelandic tholeiites have been described by Hemond *et al.* (1993)]. Also unlike samples ALV-2384-3 and 12-7, the SIE-depleted Icelandic inclusions do not have higher CaO and lower Na_2O contents than the host lava (compare Figs 2 and 9). It should be noted that Icelandic inclusions have similar Na_2O and CaO contents to inclusions in samples ALV-2384-3 and 12-7. However, in this case the host Icelandic lava has unusually high CaO and low Na_2O contents, and thus we suggest that the compositions of the host lavas are also affected by DRM processes in this case.

The effect of DRM processes on the compositions of erupted MORB lavas, such as positive Sr anomalies combined with relatively low SIE and high CaO contents, has also been identified in the most primitive pillow-rim glasses from the Ocean Drilling Program (ODP) Hole 896A (McNeill & Danyushevsky, 1996; Danyushevsky *et al.*, in preparation) and in samples collected at ~16·7°N, MAR (Silantiev & Danyushevsky, in preparation). The common occurrence of DRM processes has also been inferred from the geology of lower oceanic crust exposed as ophiolite complexes (e.g. Bedard *et al.*, 2000). The general effects of interaction between primitive melts and the lower oceanic crust with respect to the compositions of erupted lavas, such as unusually low contents of incompatible elements and positive Sr anomalies in some MORB and ophiolites, have been discussed by Elthon *et al.* (1986), Bedard (1993), Hemond *et al.* (1993) and Bedard *et al.* (2000).

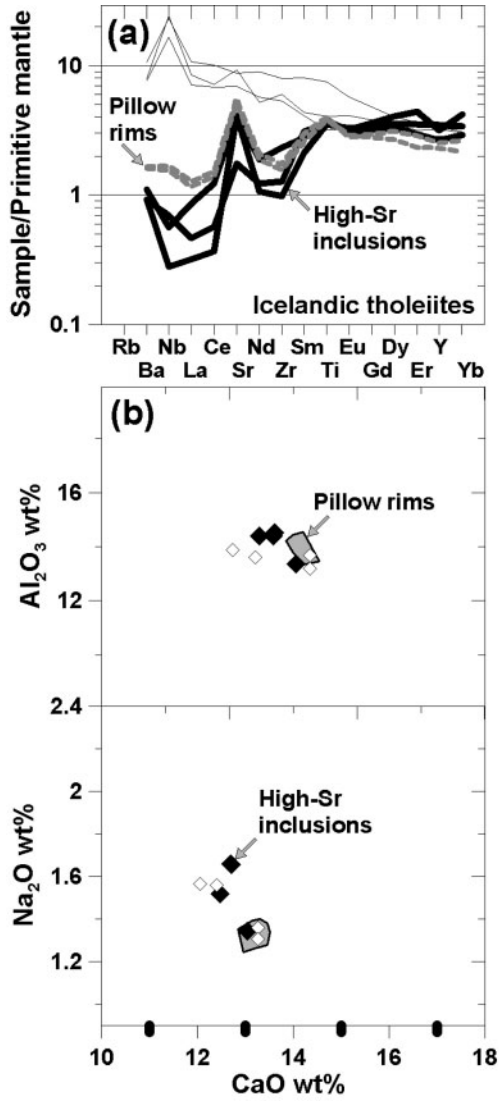

Fig. 9. Composition of melt inclusions in high-Fo olivine phenocrysts from primitive Icelandic tholeiites (Gurenko & Chaussidon, 1995). All compositions are recalculated to correct for fractionation as described in the Appendix. (a) Primitive mantle-normalized incompatible element contents of melt inclusions. Bold black lines show inclusions with positive Sr anomalies. Dashed grey lines show compositions of pillow-rim glasses of host lavas. Normalization to the primitive mantle values of Sun & McDonough (1989). (b, c) The CaO, Al_2O_3 and Na_2O contents in melt inclusions from Fig. 7a. Filled diamonds show inclusions with Sr anomalies from Fig. 7a. The fields show fractionation-corrected compositions of pillow-rim glasses from Gurenko & Chaussidon (1995). (See text for discussion.)

Concluding remarks

Summarizing the available data on anomalous melt inclusions in primitive olivine phenocrysts, we demonstrate that such inclusions are prone to localized contamination as a result of the common occurrence of DRM processes in mid-ocean ridge and subduction-related settings. As these processes are generally far less important in constraining bulk magma compositions, the compositions of the anomalous inclusions should not be used in the context of petrogenetic interpretations. Currently, most anomalous inclusions are interpreted to represent geologically significant, large-volume melts in the magmatic system, whose fractionation leads to crystallization of the host olivine phenocrysts (e.g. Kamenetsky *et al.*, 1998; Schiano *et al.*, 2000; Sobolev *et al.*, 2000). We emphasize that approaches developed for studies of bulk-rock compositions should not be automatically adopted for the study of melt inclusions. The occurrence of inclusions with unusual compositions does not necessarily imply the existence of new geologically significant magma types, as their origin may be related to DRM-type processes.

These conclusions do not undermine the importance of studies of melt inclusions in primitive phenocrysts. In suites where anomalous inclusions are common, samples containing phenocrysts with rare small inclusions may record unmodified melt compositions not associated with reaction zones. (e.g. Tavua shoshonite samples described above). All inclusions, regardless of their origin, can be used to infer the cooling histories of olivine phenocrysts (Danyushevsky *et al.*, 2002*c*). Anomalous inclusions can be used to investigate the DRM processes, which normally occur on a micro-scale only and thus cannot be identified from the study of bulk-rock compositions.

ACKNOWLEDGEMENTS

This research was supported by the Australian Research Council through Research Fellowships and Research Grants to L.V.D. and A.J.C. Stimulating discussions over the years with Dima Kamenetsky and Alex Sobolev have clarified many initial ideas and interpretations. Editorial handling and insightful suggestions by Marjorie Wilson, and comments by three anonymous reviewers, significantly improved the original manuscript. We acknowledge support of the Museum of Natural History, Washington, DC, which provided electron microprobe standards.

SUPPLEMENTARY DATA

Supplementary data for this paper are available at *Journal of Petrology* online.

REFERENCES

Bedard, J. H. (1993). Oceanic crust as a reactive filter: synkinematic intrusion, hybridization, and assimilation in an ophiolitic magma chamber, western Newfoundland. *Geology* **21**, 77–80.

Bedard, J. H. & Hebert, R. (1998). Formation of chromitites by assimilation of crustal pyroxenites and gabbros into perodititic

intrusions: North Arm Mountain massif, Bay of Islands ophiolite, Newfoundland, Canada. *Journal of Geophysical Research* **103B**, 5165–5184.

Bedard, J. H., Hebert, R., Berclaz, A. & Varfalvy, V. (2000). Syntexis and the genesis of lower oceanic crust. *Geological Society of America, Special Papers* **349**, 105–119.

Cole, J. W., Gamble, J. A., Burt, R. M., Carroll, L. D. & Shelley, D. (2001). Mixing and mingling in the evolution of andesite–dacite magmas; evidence from co-magmatic plutonic enclaves, Taupo Volcanic Zone, New Zealand. *Lithos* **59**, 25–46.

Danyushevsky, L. V. (2001). The effect of small amounts of H_2O on crystallization of mid-ocean ridge and backarc basin magmas. *Journal of Volcanology and Geothermal Research* **110**, 265–280.

Danyushevsky, L. V., Sobolev, A. V. & Falloon, T. J. (1995). North Tongan high-Ca boninite petrogenesis: the role of Samoan plume and subduction zone–transform fault transition. *Journal of Geodynamics* **20**, 219–241.

Danyushevsky, L. V., Della-Pasqua, F. N. & Sokolov, S. (2000*a*). Re-equilibration of melt inclusions trapped by magnesian olivine phenocrysts from subduction-related magmas: petrological implications. *Contributions to Mineralogy and Petrology* **138**, 68–83.

Danyushevsky, L. V., Eggins, S. M., Falloon, T. J. & Christie, D. M. (2000*b*). H_2O abundance in depleted to moderately enriched mid-ocean ridge magmas, Part I: Incompatible behaviour, implications for mantle storage, and origin of regional variations. *Journal of Petrology* **41**, 1329–1364.

Danyushevsky, L. V., Gee, M. A. M., Nisbet, E. G. & Cheadle, M. J. (2002*a*). Olivine-hosted melt inclusions in Belingwe komatiites: implications for cooling history, parental magma composition and its H_2O content. Goldschmidt Conference Abstracts 2002. *Geochimica et Cosmochimica Acta* **66**(S1), A168.

Danyushevsky, L. V., McNeill, A. W. & Sobolev, A. V. (2002*b*). Experimental and petrological studies of melt inclusions in phenocrysts from mantle-derived magmas: an overview of techniques, advantages and complications. *Chemical Geology* **183**, 5–24.

Danyushevsky, L. V., Sokolov, S. & Falloon, T. J. (2002*c*). Melt inclusions in olivine phenocrysts: using diffusive re-equilibration to determine the cooling history of a crystal, with implications for the origin of olivine-phyric volcanic rocks. *Journal of Petrology* **43**, 1651–1671.

Danyushevsky, L. V., Perfit, M. R., Eggins, S. M. & Falloon, T. J. (2003). Crustal origin for coupled 'ultra-depleted' and 'plagioclase' signatures in MORB olivine-hosted melt inclusions: evidence from the Siqueiros Transform Fault, East Pacific Rise. *Contributions to Mineralogy and Petrology* **144**, 619–637.

Davidson, J. P. & Tepley, F. J., III (1997). Recharge in volcanic systems: evidence from isotope profiles of phenocrysts. *Science* **275**, 826–829.

Della-Pasqua, F. N. (1997). Primitive ankaramitic magmas in volcanic arcs: evidence from melt inclusions. Ph.D. thesis, University of Tasmania, Hobart, 279 pp.

Della-Pasqua, F. N. & Varne, R. (1997). Primitive ankaramitic magmas in volcanic arcs: a melt inclusion approach. *Canadian Mineralogist* **35**, 291–312.

Elthon, D., Karson, J. A., Casey, J. F., Sullivan, J. & Siroky, F. X. (1986). Geochemistry of diabase dikes from the Lewis Hills Massif, Bay of Islands ophiolite: evidence for partial melting of oceanic crust in transform faults. *Earth and Planetary Science Letters* **78**, 89–103.

Gaetani, G. A. & Watson, E. B. (2000). Open system behavior of olivine-hosted melt inclusions. *Earth and Planetary Science Letters* **183**, 27–41.

Gaetani, G. A., Cherniak, D. J. & Watson, E. B. (2002). Diffusive reequilibration of CaO in olivine-hosted melt inclusions. *Geochimica et Cosmochimica Acta* **66**(15A), A254.

Gamble, J. A., Wood, C. P., Price, R. C., Smith, I. E. M., Stewart, R. B. & Waight, T. (1999). A fifty year perspective of magmatic evolution on Ruapehu Vocano, New Zealand: verification of open system behaviour in an arc volcano. *Earth and Planetary Science Letters* **170**, 301–314.

Gill, J. B. & Whelan, P. (1989). Early rifting of an oceanic island arc (Fiji) produced shoshonitic to tholeiitic basalts. *Journal of Geophysical Research* **94B**, 4561–4578.

Gioncada, A., Clocchiatti, R., Sbrana, A., Bottazzi, P., Massare, D. & Ottolini, L. (1998). A study of melt inclusions at Vulcano (Aeolian islands, Italy): insights on the primitive magmas and on the volcanic feeding system. *Bulletin of Volcanology* **60**, 286–306.

Gurenko, A. A. & Chaussidon, M. (1995). Enriched and depleted primitive melts included in olivine from Icelandic tholeiites—origin by continuous melting of a single mantle column. *Geochimica et Cosmochimica Acta* **59**, 2905–2917.

Hemond, C., Arndt, N. T., Lichtenstein, U. & Hofmann, A. W. (1993). The heterogeneous Iceland Plume: Nd–Sr–O isotopes and trace element constraints. *Journal of Geophysical Research* **98B**, 15833–15850.

Huppert, H. E. & Sparks, R. S. J. (1980). The fluid dynamics of a basaltic magma chamber replenished by influx of hot, dense ultrabasic magma. *Contributions to Mineralogy and Petrology* **75**, 279–289.

Jarosewich, E. J., Nelen, J. A. & Norberg, J. A. (1980). Reference samples for electron microprobe analyses. *Geostandards Newsletter* **4**, 257–258.

Kamenetsky, V. S. & Clocchiatti, R. (1996). Primitive magmatism of Mt. Etna: insights from mineralogy and melt inclusions. *Earth and Planetary Science Letters* **142**, 553–572.

Kamenetsky, V. S., Crawford, A. J., Eggins, S. & Muhe, R. (1997). Phenocryst and melt inclusion chemistry of near-axis seamounts, Valu Fa Ridge, Lau Basin: insight into mantle wedge melting and addition of subduction components. *Earth and Planetary Science Letters* **151**, 205–223.

Kamenetsky, V. S., Eggins, S. M., Crawford, A. J., Green, D. H., Gasparon, M. & Falloon, T. J. (1998). Calcic melt inclusions in primitive olivine at 43°N MAR: evidence for melt–rock reaction/melting involving clinopyroxene-rich lithologies during MORB generation. *Earth and Planetary Science Letters* **160**, 115–132.

Kent, A. J. R., Baker, J. A. & Wiedenbeck, M. (2002). Contamination and melt aggregation processes in continental flood basalts: constraints from melt inclusions in Oligocene basalts from Yemen. *Earth and Planetary Science Letters* **202**, 577–594.

Kogiso, T. & Hirschmann, M. M. (2001). Experimental study of leucopyroxenite partial melting and the origin of ultra-calcic melt inclusions. *Contributions to Mineralogy and Petrology* **142**, 347–360.

Lassiter, J. C., Hauri, E. H., Nikogosian, I. K. & Barsczus, H. G. (2002). Chlorine–potassium variations in melt inclusions from Raivavae and Rapa, Austral Islands: constraints on chlorine recycling in the mantle and evidence for brine-induced melting of oceanic crust. *Earth and Planetary Science Letters* **202**, 525–540.

Longerich, H. P., Jackson, S. E. & Gunther, D. (1996). Laser ablation inductively coupled plasma mass spectrometric transient signal data acquisition and analyte concentration calculation. *Journal of Analytical Atomic Spectrometry* **11**, 899–904.

Marsh, B. D. (1995). Solidification fronts and magmatic evolution. *Mineralogical Magazine* **60**, 5–40.

Marsh, B. D. (1998). On the interpretation of crystal size distribution in magmatic systems. *Journal of Petrology* **39**, 553–599.

Massare, D., Metrich, N. & Clocchiatti, R. (2002). High-temperature experiments on silicate melt inclusions in olivine at 1 atm: inference on temperatures of homogenization and H_2O concentrations. *Chemical Geology* **183**, 87–98.

McNeill, A. W. & Danyushevsky, L. V. (1996). Compositions and crystallization temperatures of primary melts for Hole 896A basalts: evidence from melt inclusion studies. In: Michael, P. J. (ed.) *Proceedings of the Ocean Drilling Program, Scientific Reports, 148*. College Station, TX: Ocean Drilling Program, pp. 21–35.

Melson, W. G., O'Hearn, T. & Jarosewich, E. J. (2002). A data brief on the Smithsonian Abyssal Volcanic Glass data file. *Geochemistry, Geophysics, Geosystems* **3**(4), doi: 10.1029/2001GC00024-9.

Metrich, N., Schiano, P., Clocchiatti, R. & Maury, R. C. (1999). Transfer of sulfur in subduction settings: an example from Batan Island (Luzon volcanic arc, Philippines). *Earth and Planetary Science Letters* **167**, 1–14.

Nielsen, R. L., Crum, J., Bourgeois, R., Hascall, K., Forsythe, L. M., Fisk, M. R. & Christie, D. M. (1995). Melt inclusions in high-An plagioclase from the Gorda Ridge: an example of the local diversity of MORB parent magmas. *Contributions to Mineralogy and Petrology* **122**, 34–50.

Perfit, M. R., Fornari, D. J., Ridley, W. I., Kirk, P. D., Casey, J., Kastens, K. A., Reynolds, J. R., Edwards, M., Desonie, D., Shuster, R. & Paradis, S. (1996). Recent volcanism in the Siqueiros transform fault: picritic basalts and implication for MORB magma genesis. *Earth and Planetary Science Letters* **141**, 91–108.

Qin, Z., Lu, F. & Anderson, A. T. (1992). Diffusive re-equilibration of melt and fluid inclusions. *American Mineralogist* **77**, 565–576.

Roedder, E. (1979). Origin and significance of magmatic inclusions. *Bulletin de Minéralogie* **102**, 487–510.

Roedder, E. (1984). *Fluid Inclusions. Mineralogical Society of America, Reviews in Mineralogy* **14**, 620 pp.

Saal, A. E., Hauri, E. H., Langmuir, C. H. & Perfit, M. R. (2002). Vapor undersaturation in primitive mid-ocean-ridge basalt and the volatile content of Earth's upper mantle. *Nature* **419**, 451–455.

Schiano, P., Eiler, J. M., Hutcheon, I. D. & Stolper, E. M. (2000). Primitive CaO-rich, silica-undersaturated melts in island arcs: evidence for the involvement of clinopyroxene-rich lithologies in the petrogenesis of arc magmas. *Geochemistry, Geophysics, Geosystems* **1**(32), doi: 10.1029/1999GC000032.

Setterfield, T. M., Eaton, P. C., Rose, W. J. & Sparks, R. S. J. (1991). The Tavua caldera, Fiji: a complex shoshonitic caldera formed by concurrent faulting and downsagging. *Journal of the Geological Society, London* **148**, 115–127.

Shibata, T., Thompson, G. & Frey, F. A. (1979). Tholeiitic and alkali basalts from the Mid-Atlantic Ridge at 43°N. *Contributions to Mineralogy and Petrology* **70**, 127–141.

Shimizu, N. (1998). The geochemistry of olivine-hosted melt inclusions in a FAMOUS basalt ALV519-4-1. *Physics of the Earth and Planetary Interiors* **107**, 183–201.

Sigurdsson, I. A., Steinthorsson, S. & Gronvöld, K. (2000). Calcium-rich melt inclusions in Cr-spinels from Borgarhraun, northern Iceland. *Earth and Planetary Science Letters* **183**, 15–26.

Sinton, C. W., Christie, D. M., Coombs, V. L., Nielsen, R. L. & Fisk, M. R. (1993). Near primary melt inclusions in anorthite phenocrysts from the Galapagos Platform. *Earth and Planetary Science Letters* **119**, 527–537.

Sinton, J. M. & Detrick, R. S. (1992). Mid-ocean ridge magma chambers. *Journal of Geophysical Research* **97B**, 197–216.

Sisson, T. W. & Bronto, S. (1998). Evidence for pressure-release melting beneath magmatic arcs from basalt at Galungnung, Indonesia. *Nature* **391**, 883–886.

Sobolev, A. V. (1996). Melt inclusions in minerals as a source of principal petrological information. *Petrology* **4**, 228–239.

Sobolev, A. V. & Hofmann, A. W. (1999). Incompatible behavior of sulfur in ultra-depleted MORB. *Ofioliti* **24**, 166.

Sobolev, A. V. & Shimizu, N. (1993). Ultra-depleted primary melt included in an olivine from the Mid-Atlantic Ridge. *Nature* **363**, 151–154.

Sobolev, A. V., Dmitriev, L. V., Barsukov, V. L., Nevsorov, V. N. & Slutsky, A. B. (1980). The formation conditions of the high-magnesian olivines from the monomineralic fraction of Luna 24 regolith. *Proceedings of the 11th Lunar Science Conference. Geochimica et Cosmochimica Acta Supplement*, Vol 1(11), 105–116.

Sobolev, A. V., Danyushevsky, L. V., Dmitriev, L. V. & Suschevskaya, N. M. (1989). High-alumina magnesian tholeiite as the primary basalt magma at midocean ridge. *Geochemistry International* **26**, 128–133.

Sobolev, A. V., Casey, J. F., Shimizu, N. & Perfit, M. (1992). Contamination and mixing of MORB primary melts: evidence from inclusions study in Siqueiros picrites. *EOS Transactions, American Geophysical Union* **73**, S336.

Sobolev, A. V., Hofmann, A. W. & Nikogosian, I. K. (2000). Recycled oceanic crust observed in 'ghost plagioclase' within the source of Mauna Loa lavas. *Nature* **404**, 986–990.

Spiegelman, M. & Kelemen, P. B. (2003). Extreme chemical variability as a consequence of channelized melt transport. *Geochemistry, Geophysics, Geosystems* **4**(336), doi: 10.1029/2002GC00036.

Sun, S.-S. & McDonough, W. F. (1989). Chemical and isotopic systematics of oceanic basalts: implications for mantle composition and processes. In: Saunders, A. D. & Norry, M. J. (eds) *Magmatism in the Ocean Basins. Geological Society, London, Special Publications* **42**, 313–345.

Tait, S. (1992). Selective preservation of melt inclusions in igneous phenocrysts. *American Mineralogist* **77**, 146–155.

Whelan, P. M., Gill, J. B., Kollman, E., Duncan, R. A. & Drake, R. E. (1985). Radiometric dating of magmatic stages in Fiji. In: Scholl, D. W. & Vallier, T. L. (eds) *Geology and Offshore Resources of Pacific Island Arcs—Tonga Region. Circum-Pacific Council for Energy and Mineral Resources Earth Science Series* **2**, 415–435.

APPENDIX: CALCULATIONS OF PARENTAL MELT COMPOSITIONS FOR MORB SAMPLES DESCRIBED IN THIS PAPER

The compositions of melt inclusions in high-Fo olivines from sample ALV-2384-3 [Siqueiros Transform Fault, East Pacific Rise (EPR); Danyushevsky *et al.*, 2003], sample 12-7 (43°N, MAR; Kamenetsky *et al.*, 1998) and samples from the Hengill swarm, Iceland (Gurenko & Chaussidon, 1995) are more primitive (e.g. have higher MgO contents) than pillow-rim glasses of those samples. To allow direct comparison between pillow-rim glass and melt inclusion compositions (Figs 2 and 9), the former have been corrected for the effect of fractionation.

Modelling the reverse of crystallization at low pressure

All calculations were performed at 0·1 MPa and melt $Fe^{2+}/Fe^{3+} = 9$ [corresponding to fO_2 values around the quartz–fayalite–magnetite (QFM) buffer]. During

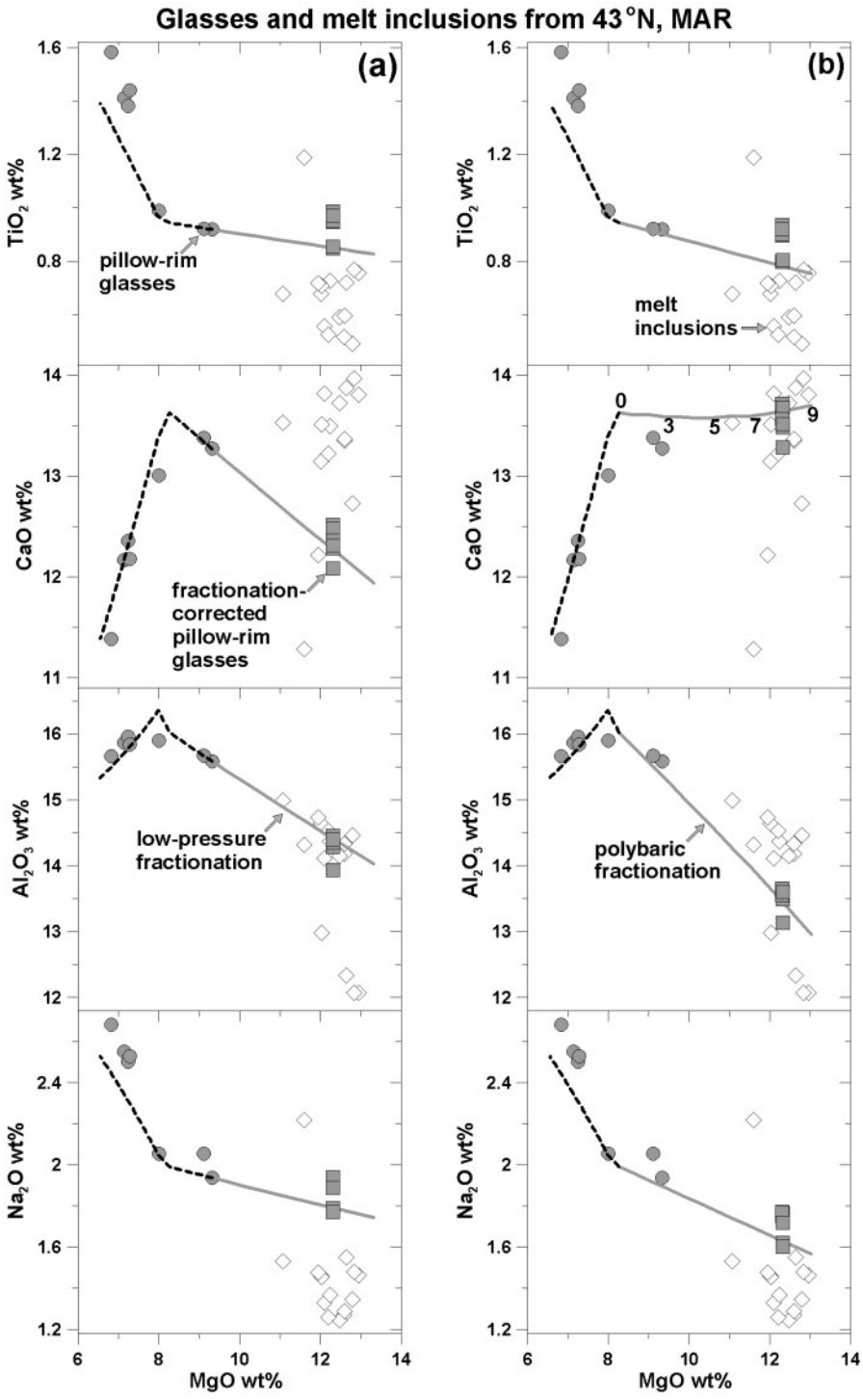

Fig. A1. Compositions of pillow-rim glasses (filled circles) and melt inclusions in high-Fo olivine phenocrysts (open diamonds) in olivine from 43°N MAR. Data are from Shibata *et al.* (1979) and Kamenetsky *et al.* (1998). Filled squares show compositions of pillow-rim glasses that have been recalculated to 12·3 wt % MgO as described in the Appendix. (a) Dashed black line represents a low-pressure (1 atm) fractionation trend of the most magnesian pillow-rim glass. At these conditions, the most magnesian glass has olivine only (plus spinel) on its liquidus. Along this fractionation path, clinopyroxene appears on the liquidus at 8·3 wt % MgO and plagioclase at 8 wt % MgO. Continuous grey line represents the reverse of olivine crystallization calculated from the composition of the most magnesian pillow-rim glass. (b) Dashed black line represents part of the low-pressure fractionation trend from (a). The high-MgO end of the trend in this figure corresponds to the moment of clinopyroxene saturation. Continuous grey line represents a polybaric olivine–clinopyroxene fractionation trend. Numbers next to the trend in the CaO–MgO plot indicate pressure in kbar. (See text for discussion.)

calculations it was assumed that all elements shown in Figs 2 and 9 are perfectly incompatible in olivine.

Pillow-rim glasses of sample ALV-2384-3 and other similar samples from the Siqueiros Transform Fault [see Perfit *et al.* (1996) and Danyushevsky *et al.* (2003) for a detailed description of these samples] have high MgO contents (9–9·5 wt %) and thus have olivine only (plus spinel) on their liquidus. This is demonstrated by increasing Al_2O_3 and CaO contents with decreasing MgO content of these glasses. Thus to account for the effects of fractionation, pillow-rim glass compositions from the Siqueiros samples have been recalculated to 11·5 wt % MgO by modelling the reverse of olivine crystallization [see Danyushevsky *et al.* (2000*a*, appendix) for a detailed description of such calculations]. Variations in the compositions of primitive pillow-rim glasses from the Siqueiros Transform have resulted in a range of compositions of the estimated parental melts shown as a field in Fig. 2b and c. The value of 11·5 wt % MgO corresponds to the average MgO content of melt inclusions, which range from 11 to 12·5 wt % (Danyushevsky *et al.*, 2003). Compositions of all inclusions have been also recalculated to 11·5 wt % MgO by modelling olivine fractionation.

Pillow-rim glasses of the Icelandic samples are also saturated in olivine only (Gurenko & Chassidon, 1995). Thus to account for the effects of fractionation, pillow-rim glass compositions from the Siqueiros samples have been recalculated to 13·3 wt % MgO by modelling the reverse of olivine crystallization. The value of 13·3 wt % MgO corresponds to the average MgO content of melt inclusions (Gurenko & Chassidon, 1995). Compositions of all inclusions have also been recalculated to 11·5 wt % MgO by modelling olivine fractionation. Re-equilibration of melt inclusions with their host phenocrysts prior to eruption ('Fe-loss'; Danyushevsky *et al.*, 2000*a*) has been taken into account by assuming that the FeO contents of the trapped inclusion compositions correspond to those along the fractionation trend of the host lavas.

Pillow-rim glasses of MORB samples from 43°N MAR (Shibata *et al.*, 1979; Kamenetsky *et al.*, 1998) are generally more evolved than glasses of the Siqueiros samples. Figure A1a demonstrates that major element compositional variations in the 43°N MAR glasses can be reasonably reproduced by modelling fractionation of the most primitive glass at 0·1 MPa. The calculations have been performed using the model of Danyushevky (2001). At these conditions the most magnesian glasses have olivine only (plus spinel) on their liquidus. Clinopyroxene appears on the liquidus at 8·3 wt % MgO, followed by plagioclase at 8 wt % MgO.

Melt inclusions in olivine phenocrysts from the 43°N MAR sample have an average MgO content of 12·3 wt %, ranging between 11 and 13 wt % (Kamenetsky *et al.*, 1998; Fig. A1a). Thus the compositions of pillow-rim glasses from this area have been recalculated to 12·3 wt % MgO by modelling the reverse of the olivine–plagioclase–clinopyroxene cotectic shown in Fig. A1a [see also Danyushevsky *et al.* (2000*b*, appendix B) for a more detailed explanation of the principles for modelling the reverse of olivine–plagioclase–clinopyroxene fractionation]. During calculation with every pillow glass composition, it has been assumed that plagioclase appeared on the liquidus at 8 wt % MgO and clinopyroxene at 8·3 wt % MgO (i.e. at higher MgO content the melt evolved in the olivine-only field). The mismatch between individual glass compositions and the forward modelling trend shown in Fig. A1a results in a range of recalculated glass compositions (Fig. A1a), which is shown as a field in Fig. 2b and c. Compositions of all inclusions have also been recalculated to 12·3 wt % MgO by modelling olivine fractionation.

Modelling the reverse of polybaric crystallization

In the 43°N MAR pillow-rim glasses, there is no direct evidence that the most magnesian compositions have crystallized at a low pressure. It is thus possible that the high-CaO compositions of melt inclusions in high-Fo olivines from this sample are related to the compositions of pillow-rim glasses by polybaric fractionation of olivine and clinopyroxene. This is supported by the presence of magnesian clinopyroxene phenocrysts in the 43°N MAR sample (Kamenetsky *et al.*, 1998)

Figure A1b shows a polybaric cotectic (from 0 to 0·9 GPa) that passes through melt inclusion compositions in the MgO–CaO plot. This cotectic corresponds to an average proportion of olivine to clinopyroxene of 3:1. In CaO–MgO space, the compositions of the melt inclusions are thus consistent with a scenario in which they represent individual melt fractions from which polybaric fractionation and mixing has produced the compositions of pillow-rim glasses from this area. This is also true for the Al_2O_3 contents of the melt inclusions. However, the NaO_2 and TiO_2 contents of the melt inclusions are lower than that required to match the compositions of pillow-rim glasses (Fig. A1b).